Prepared for submission to JCAP

Future Parameter constraints from weak lensing CMB and Galaxy Lensing Power- and Bi-spectra

Jonas Frugte[1] **P. Daniel Meerburg**[1]

[1]Van Swinderen Institute for Particle Physics and Gravity, University of Groningen, Nijenborgh 4, 9747 AG Groningen, The Netherlands

E-mail: jonasfrugte@gmail.com, p.d.meerburg@rug.nl

Contents

1 Introduction

Weak lensing has been used as a probe to constrain cosmological parameters for over a decade [21, 4, 18, 32, 5, 27]. A range of upcoming surveys, such as the survey by the Simons Observatory (SO) [2], the Legacy Survey of Space and Time (LSST) [16], and Euclid [22] aims to measure weak lensing of the cosmic microwave background (CMB) and galaxies respectively. These upcoming surveys are expected to achieve significantly higher accuracy than their predecessors, leading to tighter constraints on cosmological parameters and advancing our overall understanding of cosmology. Typically, the standard summary statistic of interest is the power spectrum (or equivalently, two-point function) of the lensing potential (as well as cross-correlations with galaxy clustering). This can be measured in terms of the lensing convergence κ, lensing shear γ, or lensing potential ψ. In the weak lensing regime they are all equivalent, in the sense that they can be directly converted into one another (appendix B). In CMB surveys, the temperature and polarization anisotropies are used to reconstruct the lensing potential [15], while with galaxies one instead calculates lensing

effects by measuring the lensing shear, which can be deduced from the ellipticity distribution of the observed galaxies [14].

Even with Gaussian initial conditions, there are significant amounts of non-Gaussianity in the weak lensing signal, especially in galaxy lensing due to it being a probe of the more recent distribution of matter [7, 30]. In addition to looking at the power spectrum, a natural next step is thus to measure weak lensing bispectra. While the bispectrum has been measured for galaxy lensing signals [33], a definitive detection of the CMB lensing bispectrum is still pending [20, 25]. Upcoming surveys, such as the ones mentioned earlier may be able to detect this signal. Therefore it is timely to consider the potential of higher order spectra to constrain cosmological parameters.

In this paper, we aim to answer this question by adopting experimental parameters similar to those of next-generation surveys. We are especially interested in seeing if approximate parameter degeneracies can be broken by combining CMB and galaxy weak lensing power- and bi-spectra. We will consider ΛCDM parameters and extensions thereof. Of particular interest are the sum of neutrino masses $\sum m_\nu$ and dark energy equation of state parameter, w_0.

The structure of this paper is as follows: we introduce relevant formulas for weak lensing statistics, nonlinear matter bispectrum, and Fisher matrix formalism in section 2. We specify details such as the fiducial values of the parameters and noise models used in section 3. Parameter constraints and signal-to-noise ratios are presented in section 4 and discussed in section 5. Useful derivations relevant to this paper can be found in the appendices. In particular, they include a derivation for the Fisher matrix formalism for the non-trivial context of bispectra with multiple tracers.

All code used to derive the results in this paper is publically available on GitHub at `https://github.com/Jonas-Frugte/fisher_calc_weak_lensing`.

2 Background

2.1 Weak lensing spectra

Radiation from cosmological objects is distorted due to gravitational lensing. Due to the low density of the cosmic web, the average deflection of a photon as it propagates through the universe is relatively weak and is thus referred to as weak lensing. Weak lensing is quantified through the deflection field $\mathbf{d}(\hat{\mathbf{n}})$ which equals the difference between the observed angle of a point in the sky and the true (unlensed) angle. This field is the gradient of the lensing potential, $\psi(\hat{\mathbf{n}})$, which is expressed as a weighted integral of the mass distribution along the line-of-sight from the observer to the source.

In the case of CMB surveys, lensing alters the statistical properties of the temperature and polarization fields and can thus be calculated by comparing the observed signal to the expected unlensed signal(see e.g. [24]). In galaxy surveys, lensing alters the ellipticities of observed galaxies. If a large enough number of galaxies are observed, this effect can be separated from the intrinsic ellipticities of the galaxies which allows us to estimate the lensing potential.

To constrain cosmological parameters we can then look at the lensing potential of the CMB, ψ_{CMB},

and of galaxy surveys, $\psi_{\rm gal}$. These are directly related to the matter power and bispectra as

$$C_\ell^{\psi_X\psi_Y} = \frac{9}{\ell^4}\Omega_m^2 H_0^4 \int_0^{\chi_*} \chi^2 \mathrm{d}\chi a(\eta_0-\chi)^{-2} W_X(\chi) W_Y(\chi) P^\delta(\ell/\chi, \eta_0-\chi), \tag{2.1}$$

$$B^{\psi_X\psi_Y\psi_Z}_{\ell\ell_1\ell\ell_2\ell\ell_3} = \sqrt{\frac{(2\ell_1+1)(2\ell_2+1)(2\ell_3+1)}{4\pi}} \begin{pmatrix} \ell_1 & \ell_2 & \ell_3 \\ 0 & 0 & 0 \end{pmatrix} \frac{27}{\ell_1^2\ell_2^2\ell_3^2}\Omega_m^3 H_0^6 \tag{2.2}$$

$$\times \int \chi^2 \mathrm{d}\chi a(\eta_0-\chi)^{-3} W_X(\chi) W_Y(\chi) W_Z(\chi) B^\delta(\{\ell_i/\chi\}, \eta_0-\chi), \tag{2.3}$$

with $X, Y, Z \in \{\mathrm{CMB}, \mathrm{gal}\}$. A derivation can be found in appendices A and B, or in the literature; see, e.g. [6]. Ω_m is the present day matter density parameter. H_0 is the present-day Hubble constant. $a(\eta)$ is the scale factor. η_0 is the conformal time today. χ is the comoving radial distance. χ_* is the distance to surface of last scattering. $P^\delta(k,\eta)$ is the matter power spectrum. $B^\delta(k_1,k_2,k_3,\eta)$ is the matter bispectrum. $W_X(\chi)$ is the window function. Finally,

$$\begin{pmatrix} \ell_1 & \ell_2 & \ell_3 \\ m_1 & m_2 & m_3 \end{pmatrix},$$

is the Wigner 3-j symbol. The difference between CMB and galaxy lensing is the window function, defined as

$$W_X(\chi) = \int_\chi^\infty \mathrm{d}\chi' p_X(\chi') \frac{\chi'-\chi}{\chi'\chi},$$

with p_X the radius distribution of the radiation source. For the CMB we take $p(\chi) = \delta(\chi-\chi_*)$. The window function presents the distribution of redshifts at which a CMB photon or galaxy photon is deflected. As a result, the CMB lensing window function is broader and peaks at lower redshift compared to the galaxy window function.

Our convention for defining the linear and non-linear matter power spectrum is

$$\langle \delta(\mathbf{k},\eta)\delta(\mathbf{k}',\eta)\rangle = (2\pi)^3\delta(\mathbf{k}+\mathbf{k}')P^\delta(\mathbf{k},\eta),$$

and for the bispectrum it is

$$\langle \delta(\mathbf{k}_1,\eta)\delta(\mathbf{k}_2,\eta)\delta(\mathbf{k}_3,\eta)\rangle = (2\pi)^3\delta(\mathbf{k}_1+\mathbf{k}_2+\mathbf{k}_3)B^\delta(k_1,k_2,k_3,\eta),$$

with δ the fractional matter density perturbation field.

2.2 Nonlinear matter bispectrum

Determining the nonlinear matter power spectrum can be done using numerical codes such as CAMB [23]. The nonlinear matter bispectrum was calculated from the power spectrum using a fitting formula based on perturbation theory in [13]. It is given by

$$B^\delta(k_1,k_2,k_3,\chi) = 2F_2(k_1,k_2,z)P^\delta(k_1,z)P^\delta(k_2,z) + 2 \text{ perm}, \tag{2.4}$$

where C^δ is the nonlinear matter power spectrum[1], and the kernel F_2 is modified from the tree level result with factors $a(k,z)$, $b(k,z)$, and $c(k,z)$:

$$F_2(k_1,k_2,z) = \frac{5}{7}a(k_1,z)a(k_2,z) + \frac{k_1^2+k_2^2}{2k_1k_2}b(k_1,z)b(k_2,z)\cos\theta + \frac{2}{7}c(k_1,z)c(k_2,z)\cos^2\theta. \tag{2.5}$$

[1] Compare to the tree level bispectrum where we instead use the linear power spectrum.

They are defined as:

$$a(k,z) = \frac{1+\sigma_8^{a_6}(z)\sqrt{0.7}Q(n_{\rm eff})(q^{a_1})^{n_{\rm eff}+a_2}}{1+(q^{a_1})^{n_{\rm eff}+a_2}}, \tag{2.6}$$

$$b(k,z) = \frac{1+0.2a_3(n_{\rm eff}+3)(q^{a_7})^{n_{\rm eff}+3+a_8}}{1+(q^{a_5})^{n_{\rm eff}+3.5+a_8}}, \tag{2.7}$$

$$c(k,z) = \frac{1+\left[\frac{4.5a_4}{1.5+(n_{\rm eff}+3)^4}\right](q^{a_5})^{n_{\rm eff}+3+a_9}}{1+(q^{a_5})^{n_{\rm eff}+3.5+a_9}}. \tag{2.8}$$

Here, $Q(n_{\rm eff})$ is given by:

$$Q(x) = \frac{4-2x}{1+2^{x+1}}. \tag{2.9}$$

The effective spectral index of the linear power spectrum is defined as:

$$n_{\rm eff} \equiv \frac{d\ln P_{\rm lin}^{\delta}(k)}{d\ln k}. \tag{2.10}$$

Additionally, q is given by:

$$q = \frac{k}{k_{\rm NL}}, \tag{2.11}$$

where $k_{\rm NL}$ is the scale at which nonlinearities become significant, satisfying:

$$4\pi k_{\rm NL}^3 P_{\rm lin}^{\delta}(k_{\rm NL},0) = 1. \tag{2.12}$$

The coefficients a_i are:

$$\begin{aligned} &a_1 = 0.484, \quad a_2 = 3.740, \quad a_3 = -0.849, \quad a_4 = 0.392, \\ &a_5 = 1.013, \quad a_6 = -0.575, \quad a_7 = 0.128, \quad a_8 = -0.722, \quad a_9 = -0.926. \end{aligned}$$

2.3 Fisher matrix analysis

The signal-to-noise (SNR) and parameter constraints are obtained through a Fisher matrix analysis as is standard in cosmology[12]. A full derivation of the equations used below can be found in appendix C. The auto- and cross- power spectrum Fisher matrix is given as

$$F_{\alpha\beta} = \sum_{\ell}\sum_{XY}\sum_{X'Y'}(2\ell+1)\partial_\alpha C_\ell^{XY}(C^{-1})_\ell^{XX'}(C^{-1})_\ell^{YY'}\partial_\beta C_\ell^{X'Y'},$$

where

$$C_\ell := \begin{pmatrix} C_\ell^{\psi_\kappa\psi_\kappa} & C_\ell^{\psi_\kappa\psi_\gamma} \\ C_\ell^{\psi_\kappa\psi_\gamma} & C_\ell^{\psi_\gamma\psi_\gamma} \end{pmatrix}.$$

For the bispectra we instead have

$$F_{\alpha\beta} = \sum_{\ell_1\le\ell_2\le\ell_3}\frac{\mathcal{P}_{\ell_1\ell_2\ell_3}}{6}\sum_{XYZ}\sum_{X'Y'Z'}\partial_\alpha B_{\ell_1\ell_2\ell_3}^{XYZ}(C^{-1})_{\ell_1}^{XX'}(C^{-1})_{\ell_2}^{YY'}(C^{-1})_{\ell_3}^{ZZ'}\partial_\beta B_{\ell_1\ell_2\ell_3}^{X'Y'Z'},$$

with $\mathcal{P}_{\ell_1\ell_2\ell_3}$ defined as the number of distinct permutations that can be made with $\ell_1\ell_2\ell_3$. When only considering auto spectra the formulas simplify to:

$$F_{\alpha\beta} = \sum_{\ell}\sum_{XY}\sum_{X'Y'}\frac{2\ell+1}{2}\frac{\partial_\alpha C_\ell^{XX}\partial_\beta C_\ell^{XX}}{(C_\ell^{XX})^2},$$

and (for bispectra, assuming Gaussian, diagonal, covariance)

$$F_{\alpha\beta} = \sum_{\ell_1 \leq \ell_2 \leq \ell_3} \frac{\mathcal{P}_{\ell_1\ell_2\ell_3}}{6} \frac{\partial_\alpha B^{XXX}_{\ell_1\ell_2\ell_3} \partial_\beta B^{XXX}_{\ell_1\ell_2\ell_3}}{C^{XX}_{\ell_1} C^{XX}_{\ell_2} C^{XX}_{\ell_3}}.$$

If only some fraction of the sky, $f_{\rm sky}$, is measured, all Fisher matrices are multiplied by $f_{\rm sky}$ [30].

3 Calculation Details

Our fiducial cosmology is based on the Planck results [3] (see table 1). Throughout this paper we consider two priors. The first we refer to as our "weak prior" and is similar to the one used in [27] (see table 1). This prior only restricts $\Omega_b h^2$ and n_s significantly. The purpose of the weak prior is as follows. The power spectra, in particular, exhibit complete insensitivity to certain parameters. Consequently, relying solely on them to constrain the entire cosmological model results in very poor constraints. Future lensing surveys will of course use information from surveys measuring other statistics such as galaxy distributions or primary CMB anisotropies, so these poor constraints are not representative of what stage 3 and 4 experiments could achieve. By adding a prior our calculations become more realistic. Additionally, by having the prior be conservative, it stays clear how the different lensing spectra complement each other. The other prior we will use is based on the CMB temperature and E-mode polarization cross- and auto-powerspectra from $\ell = 30$ to $\ell = 2000$. With the same noise values as used for the CMB weak lensing spectra. These results will be more realistic and serve to test whether weak lensing spectra are able to further tighten constraints in the presence of surveys measuring more standard statistics (such as the primary CMB anisotropies) with similar noise values.

parameter	**notation**	**fiducial value**	**σ of weak prior**	**σ of $T+E$ prior**
Hubble constant	H_0	67.4 km/s/Mpc	17.3	1.21
Physical baryon density parameter	$\Omega_b h^2$	0.0223	0.0005	0.000057
Physical cold dark matter density parameter	$\Omega_c h^2$	0.119	0.288	0.00083
Scalar spectral index	n_s	0.965	0.02	0.0025
Reionization depth	τ	0.063	0.063	0.0013
Amplitude of primordial scalar fluctuations	A_s	2.13×10^{-9}	1×10^{-9}	5.5×10^{-11}
Sum of neutrino masses	$\sum m_\nu$	0.06	∞	0.22
Dark energy equation of state parameter	w_0	-1	∞	0.058

Table 1. Cosmological parameters varied (ΛCDM + $w_0 + m_\nu$). We use a prior similar to the one used by the Planck weak lensing results [27] which essentially only restricts $\Omega_b h^2$ and n_s significantly.

This paper considers noise levels for "stage 3" and "stage 4" weak lensing surveys. Values can be found in table 2, including the experiments they are representative of. A comparison of the noise power spectra to the lensing power spectra are shown in figure 1. Effectively, for galaxy lensing, the power spectrum is signal-dominated up until $\ell \sim 200$ (stage 3) and $\ell \sim 700$ (stage 4). For CMB lensing, the power spectrum is signal-dominated for $\ell \sim 300$ (stage 3) and $\ell \sim 1000$ (stage 4).

CMB lensing noise is estimated using the quadratic estimator from [24]. The parameters characterizing the noise levels are beam width, σ, polarization white noise, Δ_P, and temperature white noise Δ_T. We take $\Delta_T = \Delta_P/\sqrt{2}$ throughout. Galaxy lensing is determined by measuring lensing shear (see appendices A and D). The noise in this measurement is dominated by scale-independent

source	survey stage	noise vals	comparable experiments
CMB	stage 3	$\sigma = 1'$, $\Delta_P = 6'$ μK	Advanced ACTPol, SPT-3G
	stage 4	$\sigma = 3'$, $\Delta_P = 1'$ μK	CMB-S4, LiteBIRD
galaxies	stage 3	$\sigma_{\rm rms} = 0.3$, $n_g = 5 {\rm arcmin}^{-2}$	DES, KiDS
	stage 4	$\sigma_{\rm rms} = 0.3$, $n_g = 30 {\rm arcmin}^{-2}$	LSST, Euclid

Table 2. Noise levels considered for weak lensing of galaxies and the CMB. σ (beam width) and Δ_P (polarization white noise) describe CMB survey specifications, while $\sigma_{\rm rms}$ (intrinsic galaxy ellipticity) and n_g (observed galaxy density) refer to galaxy shear surveys.

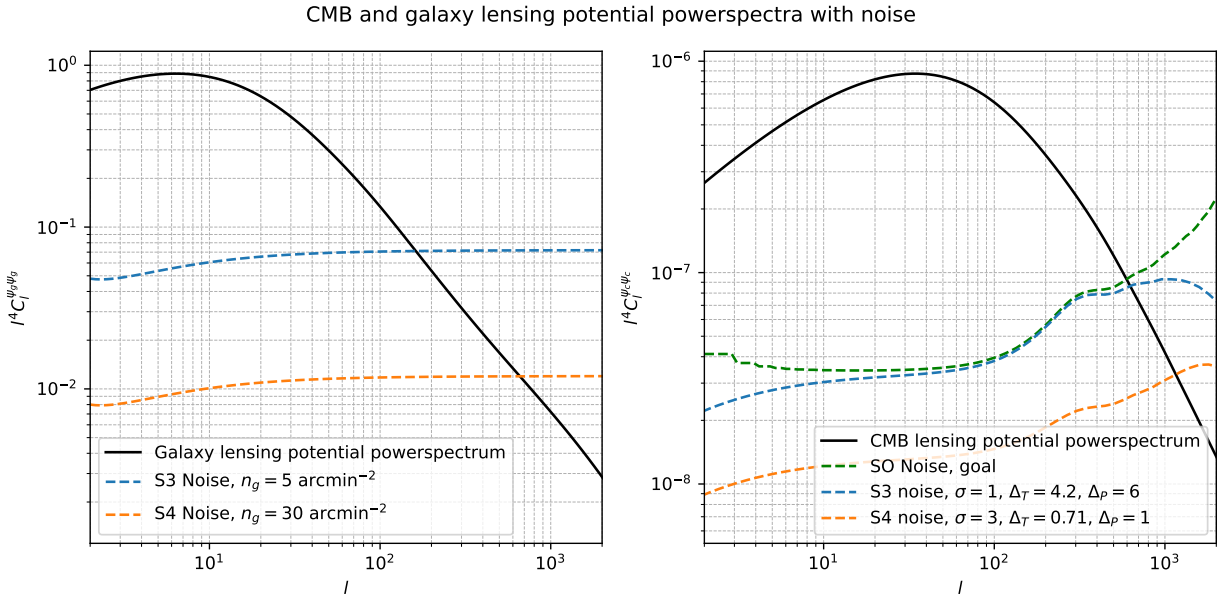

Figure 1. CMB (right) and galaxy (left) lensing potential power spectra compared to associated experimental noise. Current (stage 3) noise values are displayed as well as near future (stage 4) noise values. The CMB lensing experiment uses only polarization. CMB noise values are chosen in accordance with [25]. For comparison we also how the noise reconstruction for the Simons Observatory. Shear noise values are chosen to be similar to e.g. Euclid measurements for stage 4 and e.g. KiDS for stage 3.

shot noise and has associated noise power spectrum $N_l^{\rm shear} = \sigma_{\rm rms}^2/n_g$, [6]. n_g is the amount of galaxies observed per unit angle. The noise power spectrum for the lensing potential then equals

$$N_\ell^{\text{lens. potential}} = \frac{(\ell-1)\ell(\ell+1)(\ell+2)}{4} N_\ell^{\rm shear}.$$

In all cases we assume that the proportion of the sky surveyed, $f_{\rm sky}$, equals 0.5. For parameter constraints, we will consider only stage 4 noise levels.

The redshift distribution of the observed galaxies is commonly parameterized as [6]

$$n(z) \propto z^a \exp\left[-\left(\frac{z}{z_0}\right)^b\right].$$

We choose the parameter combination $a = 2$, $b = 3/2$ and $z_0 = 0.64$ which is similar to the expected distributions of Euclid, (which will probe primarily in the 0.2 - 2.6 redshift range [11]) and the LSST

mission (which has $a \approx 2$, $b \approx 1$, and $z_0 \approx 0.3$ from predictions for the obtained data [17]). For simplicity, we do not implement a tomographic binning of the source galaxies, and instead model the population with a single effective redshift distribution.

Derivatives are calculated with a central difference formula (see appendix E for convergence). To check the accuracy of our results we calculated constraints for similar experimental parameters as in references [27, 30, 1, 26] and found good agreement in all cases.

4 Results

Lensing power spectra have high signal-to-noise in all cases. The signal-to-noise of the CMB and galaxy lensing bispectra versus the maximum multipole moment measured is shown in figure 2. In the absence of systematics, shear bispectra can be detected at high signal-to-noise with both stage 3 and stage 4 experiments. CMB lensing bispectra could be detectable by a stage 3 experiment (see e.g. ref. [20] for the effect of noise biases) and with high signal-to-noise with a stage 4 experiment. CMB S/N results match those of reference [25].

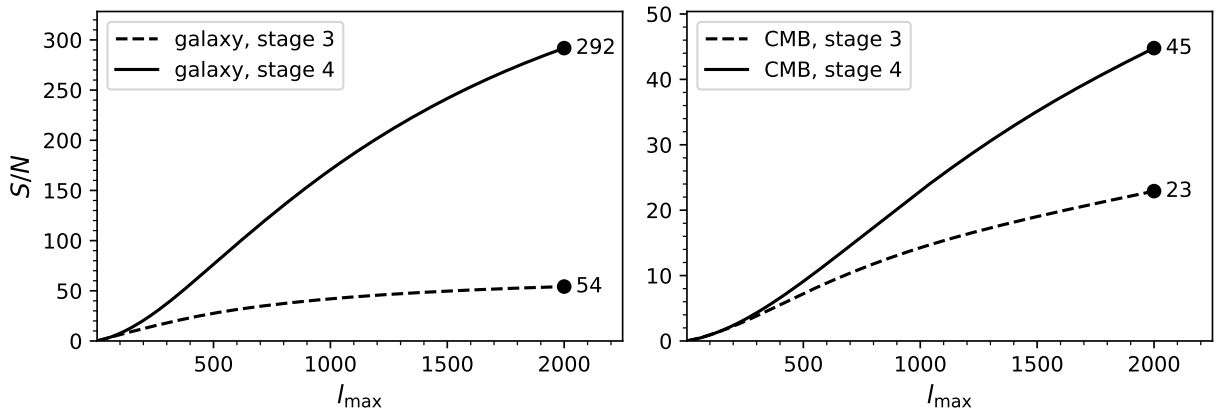

Figure 2. Signal-to-noise ratios for galaxy lensing (left) and CMB lensing (right) for stage 3 (dashed) and stage 4 (not dashed) surveys as a function of maximum multipole measured. The minimum multipole is always $l_{\rm min} = 2$. The multipole range used for CMB lensing reconstruction is $2 \leq \ell \leq 10^4$. Using a more conservative range such as $30 \leq \ell \leq 5000$ used to calculate Simons Observatory noise curves don't significantly affect the results.

Next, we consider cosmological parameter constraints. We include both the power spectrum and the bispectrum of the weak lensing. We look at two extension of ΛCDM, m_ν and w_0 as well as the derived parameters σ_8, and Ω_m. Constraints on the full set of ΛCDM parameters can be found found in appendix F. Results shown include marginalization over all parameters. Figures 3 and 5 show confidence ellipses from stage 4 CMB and galaxy lensing surveys with the weak prior, respectively. Figures 4 and 6 show confidence ellipses in the case of our CMB $T + E$ prior. Table 3 lists all forecasted constraints .

Constraints are significantly improved by including bispectrum information in nearly all cases when using weak priors. When including the CMB $T + E$ priors, both the CMB lensing power- and

bispectra significantly improve prior constraints, however combining them doesn't lead to significant improvements compared to only using lensing power spectra. For galaxy lensing, the power- and bispectra yield nearly identical improvements compared to the CMB $T + E$ prior. In this case, combining both statistics leads to significantly tighter constraints (in contrast to CMB lensing). When combining CMB and galaxy lensing we see that the bispectrum is slightly less competitive than the lensing power spectrum, but can still significantly improve constraints compared to only using the lensing power spectrum.

Furthermore, it is clear that, in general, combining CMB and galaxy lensing surveys also leads to significant improvements in constraining power, even in the case of the CMB $T + E$ prior. The improvement is strongest for the neutrino constraint.

Besides these obvious findings, we make several other conclusions:

- Lensing powers pectra alone are not sufficient to competitively constrain $\Lambda\text{CDM} + w_0 + m_\nu$ without priors, even in the case of stage 4 surveys.
- For lower noise values (in particular for stage 4 noise) the bispectra becomes increasingly important compared to the powerspectra. The lensing bispectra are directly related to the amount of non-gaussianity in the matter distribution. As noise levels becomes lower, we are are able to measure the matter distribution on small enough scales where nonlinear matter evolution becomes apparent. Additionally, for galaxy lensing, the window function peaks at earlier redshifts than compared to CMB lensing. The bispectrum is largest at late times, and thus the galaxy lensing bispectrum is significantly easier to detect and is better at constraining parameters then the CMB lensing bispectrum.
- The information from bispectra is sensitive to cosmology in a different way than that of the power spectra. The main parameter combinations where approximate degeneracies are broken are $(n_s, \Omega_b h^2)$, $(\Omega_b h^2, H_0)$, $(\Omega_c h^2, H_0)$, $(\Omega_c h^2, \Omega_b h^2)$ $(n_s, \Omega_c h^2)$, (m_ν, H_0), (m_ν, n_s), $(A_s, \Omega_b h^2)$ (see also appendix F). This means that even if stage 4 surveys aren't able to reach the noise levels assumed in this paper, the bispectra will likely still lead to significantly tighter constraints.
- Stage 4 galaxy weak lensing surveys generally contain more information than CMB surveys.

weak priors										
		CMB lensing			Gal. lensing			CMB × Gal. lensing		
Par	prior	C_ℓ	$B_{\ell_1\ell_2\ell_3}$	$C_\ell + B_{\ell_1\ell_2\ell_3}$	C_ℓ	$B_{\ell_1\ell_2\ell_3}$	$C_\ell + B_{\ell_1\ell_2\ell_3}$	C_ℓ	$B_{\ell_1\ell_2\ell_3}$	$C_\ell + B_{\ell_1\ell_2\ell_3}$
m_ν	1.00e+01	2.82e-01	1.13e+00	2.26e-01	2.60e-01	4.07e-01	1.85e-01	9.54e-02	1.81e-01	6.46e-02
w_0	1.00e+01	5.42e-01	1.44e+00	3.87e-01	2.14e-01	1.28e-01	3.22e-02	1.51e-01	1.13e-01	2.45e-02
σ_8	2.46e+00	1.18e-01	1.95e-01	5.69e-02	5.36e-02	5.43e-02	1.73e-02	3.48e-02	3.32e-02	9.20e-03
Ω_m	6.70e-01	1.95e-01	1.84e-01	7.73e-02	7.57e-02	5.88e-02	1.81e-02	5.15e-02	3.76e-02	8.57e-03
CMB $T + E$ priors										
		CMB lensing			Gal. lensing			CMB × Gal. lensing		
Par	prior	C_ℓ	$B_{\ell_1\ell_2\ell_3}$	$C_\ell + B_{\ell_1\ell_2\ell_3}$	C_ℓ	$B_{\ell_1\ell_2\ell_3}$	$C_\ell + B_{\ell_1\ell_2\ell_3}$	C_ℓ	$B_{\ell_1\ell_2\ell_3}$	$C_\ell + B_{\ell_1\ell_2\ell_3}$
m_ν	2.16e-01	5.28e-02	1.21e-01	5.22e-02	1.48e-01	1.49e-01	1.12e-01	1.88e-02	1.02e-01	1.62e-02
w_0	5.78e-02	4.19e-02	5.30e-02	4.19e-02	4.66e-02	4.77e-02	2.55e-02	3.35e-02	4.33e-02	1.99e-02
σ_8	1.55e-02	1.06e-02	1.50e-02	1.06e-02	1.18e-02	1.21e-02	8.18e-03	8.99e-03	1.19e-02	5.28e-03
Ω_m	1.50e-02	1.20e-02	1.46e-02	1.20e-02	1.34e-02	1.23e-02	9.32e-03	1.13e-02	1.19e-02	6.16e-03

Table 3. Parameter constraints for different combinations of weak lensing information. C stands for powerspectra, and B for bispectra. All surveys are assumed to be stage 4 surveys with multipole range $2 \leq \ell \leq 2000$. We use the weak and CMB priors described in table 1.

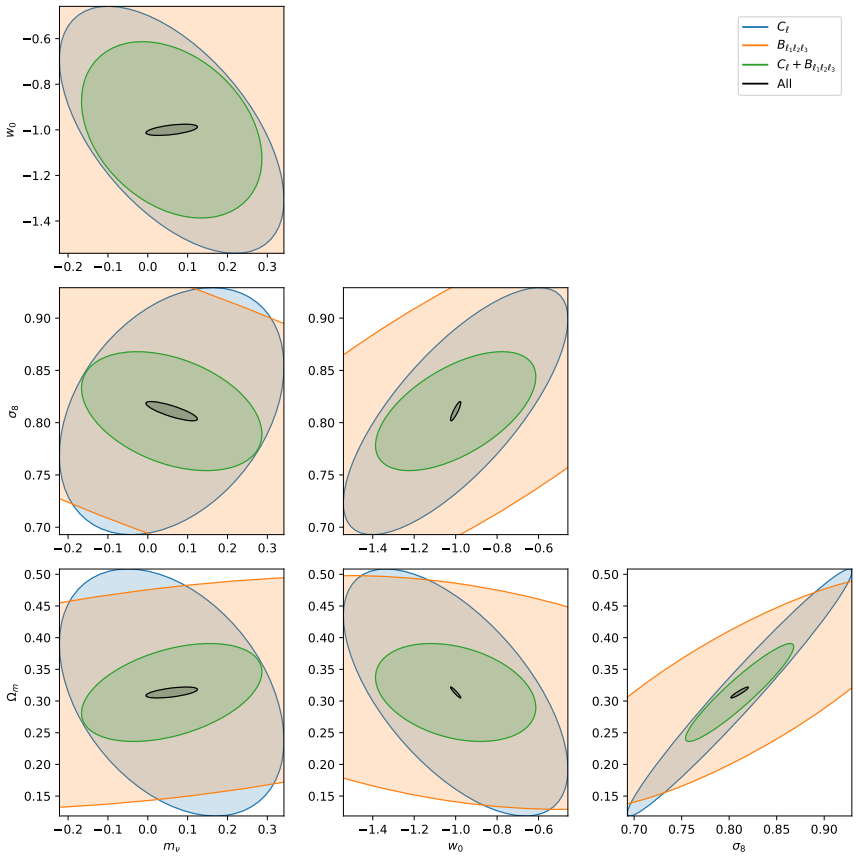

Figure 3. Parameter constraints and confidence ellipses for μ_ν, w_0, σ_8, and Ω_m. Using "stage 4" noise with multipole range from 2 to 2000. The colored plots show CMB lensing power- and/or bispectrum constraints. We use the weak priors listed in table 1. The confidence ellipses are for 1σ certainty. They show approximate degeneracies in the information gained from a survey if they are "stretched". When the information of ellipses with degeneracies in different directions is combined, the degeneracies are removed and the constraints typically becomes much better on the relevant parameters. The black plots show the constraints using all lensing information, i.e. CMB lensing spectra, galaxy lensing spectram, and all cross spectra.

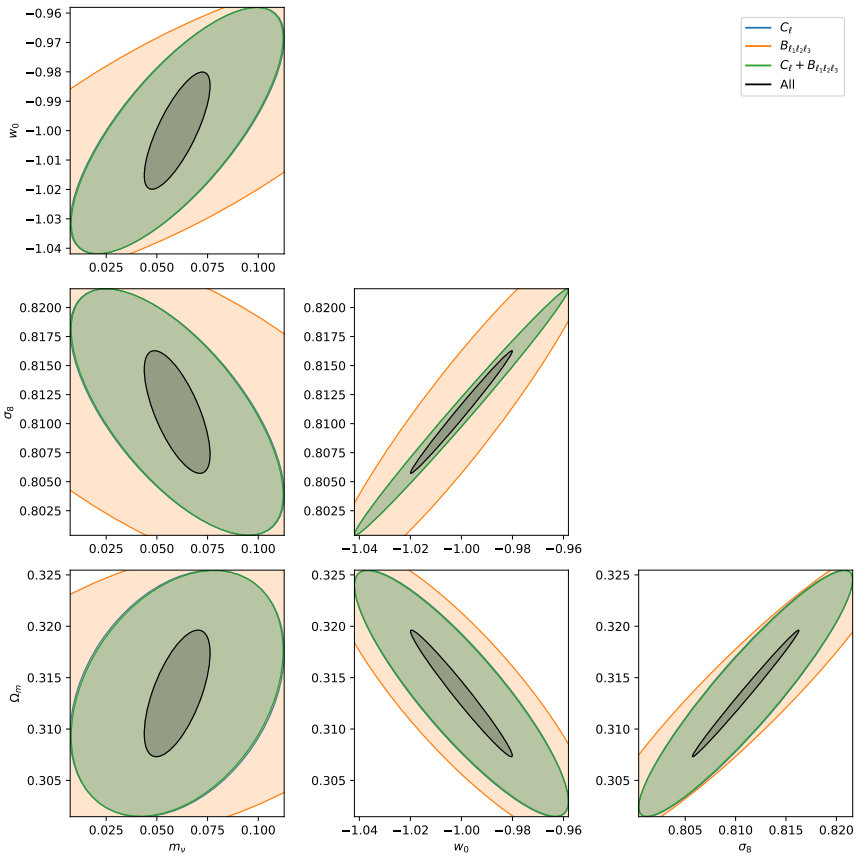

Figure 4. Same as figure 3, except we use the CMB temperature and polarization based priors listed in table 1.

5 Discussion and conclusion

In this work, we have presented parameter forecasts from CMB lensing and galaxy lensing power- and bispectra, considering experimental parameters representative of Stage 3 and Stage 4 CMB and galaxy surveys. Our analysis shows that while lensing power spectra are well detectable, the inclusion of bispectra generally offers significant improvements when considering parameter constraints. Notably, both CMB and galaxy bispectra are found to be measurable, even with Stage 3 experimental noise levels.

The primary impact of incorporating bispectrum information is a tightening of cosmological parameter constraints, particularly for parameters like H_0, σ_8, and Ω_m, and in breaking key parameter degeneracies. We found that for sufficiently low noise levels, characteristic of Stage 4 surveys, the bispectra themselves can offer constraining power comparable to or even exceeding that of the power spectra, due to a more favorable scaling of information content with the maximum usable multipole[2]. Furthermore, the combination of CMB and galaxy lensing probes, especially when both power spectra and bispectra are utilized, further enhances constraints and aids in mitigating degeneracies. However, lensing power spectra alone, even for Stage 4 surveys, appear insufficient to competitively constrain an 8-parameter $\Lambda\mathrm{CDM} + w_0 + \sum m_\nu$ model without priors.

[2]The multipole at which the noise power spectrum starts exceeding the cosmological power spectrum.

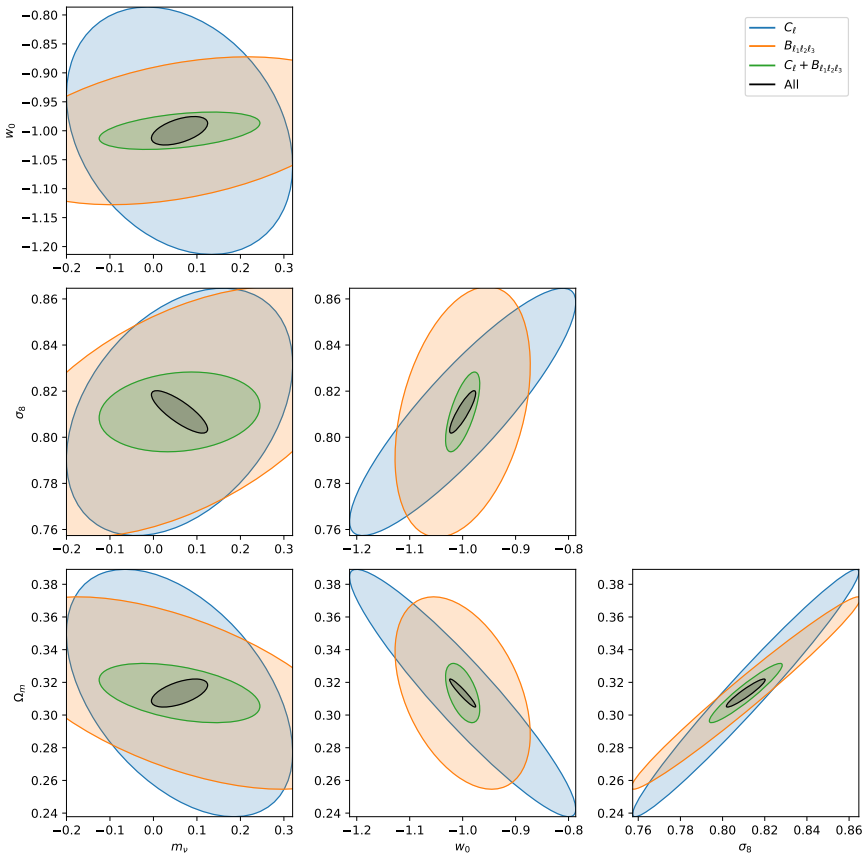

Figure 5. Same as figure 3, except here the colored plots show galaxy lensing constraints.

There are a number of limitations to the results presented in this paper. The limitations inherent to the Fisher matrix formalism and to non-physical noise models such as those considered in this paper are already well known. The main limitations specific to this work are:

- The fitting formula used for the nonlinear matter bispectrum (from [13]) has an estimated accuracy of only up to about 10 percent. This intrinsic inaccuracy in the model for B^δ will propagate to the lensing bispectra.

- Certain cosmological parameters that affect nonlinear large-scale structure, such as neutrino masses, likely alter the fitting parameters of the matter bispectrum formula when varied. In the literature, this is currently not considered, which can make the derivatives of the bispectrum with respect to these cosmological parameters less accurate.

- We assumed throughout this paper that surveys would measure multipoles as low as $\ell = 2$. However, our analytical formulas to calculate lensing spectra utilize the Limber approximation, which is only robust for $\ell \gtrsim 50$. Avoiding the Limber approximation would complicate calculations, requiring knowledge of unequal-time matter power and bispectra, and would be computationally much more demanding due to the need to evaluate double integrals instead of single integrals. With the methods used in this paper, recalculating Fisher matrices without the Limber approximation would not be feasible, even if unequal-time matter spectra

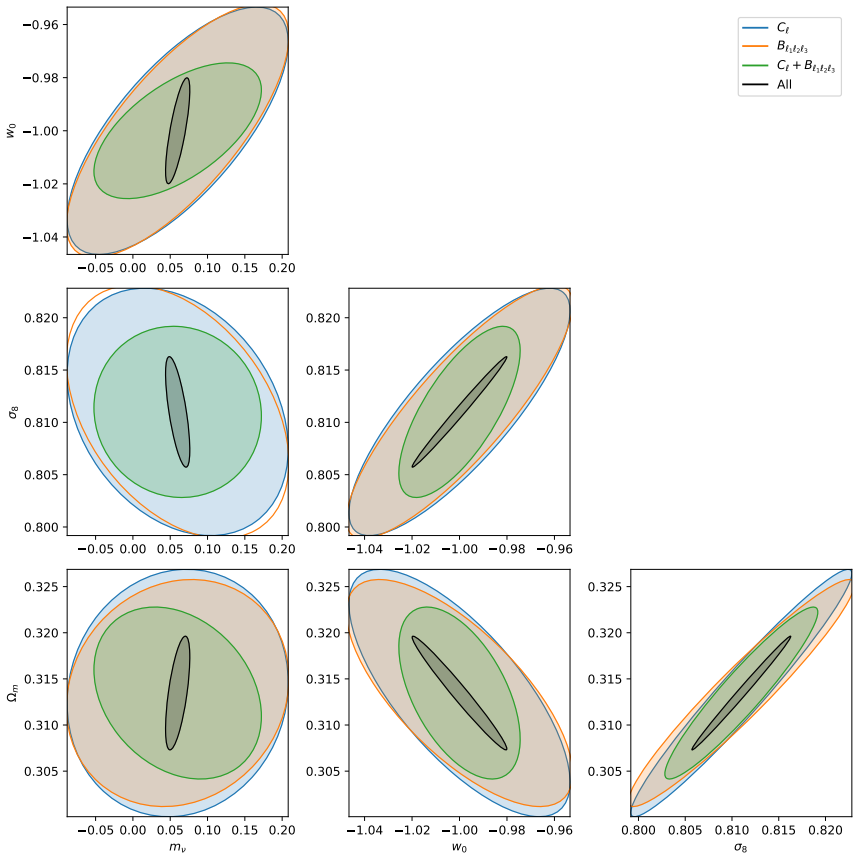

Figure 6. Same as figure 4, except here the colored plots show galaxy lensing constraints.

were readily available. Methods such as those explored in reference [9] might offer a path to address this.

- As noted in appendix C, the Gaussian approximation was used for the covariance of the spectra estimators, i.e. we ignored any contributions not arising from standard Wick contractions. A next step could be to account for these additional contributions, perhaps through N-body and ray-tracing simulations. Notably, such simulations could potentially also allow for a more accurate calculation of the lensing spectra themselves, without relying on fitting formulas for the matter bispectrum or the Limber approximation, depending on simulation accuracy. This might also explain the fact that in some instances the bispectra appear more constraining compared to the power spectra.

- The CMB lensing noise was estimated via a quadratic estimator. While standard, such estimators may not be strictly optimal, especially with complex foregrounds or non-Gaussianities. Better estimators exist; for example, the iterative estimator developed in [29] can lead to a significantly better signal-to-noise ratio for the CMB lensing bispectrum, as shown in [25]. Using such an iterative estimator may also result in the CMB bispectrum being able to significantly improve parameter constraints when combined with lensing power spectra and a CMB $T + E$ prior.

- To calculate the Fisher matrices, derivatives of the lensing spectra with respect to cosmo-

logical parameters were computed using a central difference formula. This introduces errors (estimated at most a few percent, though larger for neutrino mass derivatives, see appendix E). Functions such as the matter power spectrum and fitting parameters for the matter bispectrum were approximated using pre-generated data and interpolation, also introducing errors of at most a few percent. Currently, these numerical errors are not considered significant because this paper primarily aims to provide a qualitative understanding of the utility of CMB and galaxy weak lensing spectra. However, for precise quantitative results, these factors would need to be revisited and improved.

- A recent paper [28] has shown that the Born approximation used to derive the formulas for the lensing power and bispectra, is no longer negligible for the lensing bispectrum. The post-Born corrections calculated in that paper only changed the lensing power spectra by $\leq 0.2\%$, while for the bispectra this effect was much larger, in particular for folded configurations. For future work it would thus be worthwile to analyze how these post-Born corrections affect the results presented in this paper.

Despite these limitations, this work provides valuable insight into the potential of future weak lensing surveys. Addressing these limitations will be crucial for obtaining robust cosmological constraints from upcoming observational data.

References

[1] Kevork N. Abazajian et al. *CMB-S4 Science Book, First Edition*. 2016. arXiv: 1610.02743 [astro-ph.CO]. URL: https://arxiv.org/abs/1610.02743.

[2] PAR Ade, J Aguirre, Z Ahmed, et al. "The Simons Observatory: science goals and forecasts". In: *Journal of Cosmology and Astroparticle Physics* 2019.02 (2019), p. 056.

[3] N. Aghanim et al. "Planck2018 results: VI. Cosmological parameters". In: *Astronomy and Astrophysics* 641 (Sept. 2020), A6. ISSN: 1432-0746. DOI: 10.1051/0004-6361/201833910. URL: http://dx.doi.org/10.1051/0004-6361/201833910.

[4] D. Bacon, A. Refregier, and R. Ellis. "Detection of weak gravitational lensing by large-scale structure". In: *Monthly Notices of the Royal Astronomical Society* 318 (2000), pp. 625–640.

[5] Matthias Bartelmann and Peter Schneider. "Weak gravitational lensing". In: *Physics Reports* 340 (2001), pp. 291–472.

[6] Matthias Bartelmann and Peter Schneider. "Weak Gravitational Lensing". In: *Physics Reports* 340.4-5 (2001), pp. 291–472. DOI: 10.1016/S0370-1573(00)00082-X.

[7] F. Bernardeau, L. Van Waerbeke, and Y. Mellier. "Weak lensing statistics as a probe of non-Gaussian initial conditions". In: *Astronomy & Astrophysics* 322 (1997), pp. 1–18.

[8] George Casella and Roger L. Berger. *Statistical Inference*. 2nd. Duxbury Pacific Grove, CA, 2002. ISBN: 9780534243128.

[9] Shu-Fan Chen, Hayden Lee, and Cora Dvorkin. "Precise and accurate cosmology with CMB×LSS power spectra and bispectra". In: *JCAP* 05 (2021), p. 030. DOI: 10.1088/1475-7516/2021/05/030. arXiv: 2103.01229 [astro-ph.CO].

[10] Asantha Cooray and Wayne Hu. "Weak Gravitational Lensing Bispectrum". In: *The Astrophysical Journal* 548.1 (Feb. 2001), pp. 7–18. ISSN: 1538-4357. DOI: 10.1086/318660. URL: http://dx.doi.org/10.1086/318660.

[11] Euclid Collaboration: G. Desprez, S. Paltani, J. Coupon, et al. "Euclid Preparation - X. The Euclid Photometric-Redshift Challenge". In: *Astronomy and Astrophysics* 644 (2020), A31. DOI: 10.1051/0004-6361/202039403. URL: https://www.aanda.org/articles/aa/pdf/2020/12/aa39403-20.pdf.

[12] Scott Dodelson and Fabian Schmidt. *Modern Cosmology*. 2nd. Elsevier, 2020. ISBN: 978-0-12-815948-4.

[13] Hector Gil-Marin et al. "An improved fitting formula for the dark matter bispectrum". In: *Journal of Cosmology and Astroparticle Physics* 2012.02 (2012), p. 047. DOI: 10.1088/1475-7516/2012/02/047. arXiv: 1111.4477 [astro-ph.CO].

[14] Henk Hoekstra and Bhuvnesh Jain. "Weak Gravitational Lensing and Its Cosmological Applications". In: *Annual Review of Nuclear and Particle Science* 58.1 (2008), pp. 99–123.

[15] Wayne Hu and Takemi Okamoto. "Mass Reconstruction with Cosmic Microwave Background Polarization". In: *The Astrophysical Journal* 574.2 (Aug. 2002), pp. 566–574. ISSN: 1538-4357. DOI: 10.1086/341110. URL: http://dx.doi.org/10.1086/341110.

[16] Ž. Ivezić, S. M. Kahn, J. A. Tyson, et al. "LSST: From Science Drivers to Reference Design and Anticipated Data Products". In: *The Astrophysical Journal* 873.2 (2019), p. 111.

[17] Steven M. Kahn, Justin R. Bankert, Srinivasan Chandrasekharan, et al. "LSST System Performance". In: *LSST Science Book, Version 2.0*. Accessed: 2025-02-11. 2009. URL: https://www.lsst.org/sites/default/files/docs/sciencebook/SB_3.pdf.

[18] N. Kaiser, G. Wilson, and G. Luppino. "Large-Scale Cosmic Shear Measurements". In: *arXiv preprint astro-ph/0003338* (2000).

[19] Alba Kalaja, P. Daniel Meerburg, and William R. Pimentel Guilherme L.and Coulton. "Fundamental limits on constraining primordial non-Gaussianity". In: *Journal of Cosmology and Astroparticle Physics* 2021.04 (Apr. 2021), p. 050. ISSN: 1475-7516. DOI: 10.1088/1475-7516/2021/04/050. URL: http://dx.doi.org/10.1088/1475-7516/2021/04/050.

[20] Alba Kalaja et al. "The reconstructed CMB lensing bispectrum". In: *Journal of Cosmology and Astroparticle Physics* 2023.04 (Apr. 2023), p. 041. ISSN: 1475-7516. DOI: 10.1088/1475-7516/2023/04/041. URL: http://dx.doi.org/10.1088/1475-7516/2023/04/041.

[21] Martin Kilbinger. "Cosmology with cosmic shear observations: a review". In: *Reports on Progress in Physics* 78.8 (2015), p. 086901. DOI: 10.1088/0034-4885/78/8/086901. URL: https://arxiv.org/abs/1411.0115.

[22] R. Laureijs and others (Euclid Collaboration). *Euclid Definition Study Report*. ESA/SRE(2011)12. 2011. arXiv: 1110.3193.

[23] Antony Lewis, Anthony Challinor, and Anthony Lasenby. "Efficient computation of cosmic microwave background anisotropies in closed FRW models". In: *The Astrophysical Journal* 538 (2000), pp. 473–476.

[24] Abhishek S Maniyar et al. "Quadratic Estimators for CMB Weak Lensing". In: *arXiv preprint arXiv:2101.12193* (2021).

[25] Toshiya Namikawa. "CMB lensing bispectrum from nonlinear growth of the large scale structure". In: *Physical Review D* 93.12 (June 2016). ISSN: 2470-0029. DOI: 10.1103/physrevd.93.121301. URL: http://dx.doi.org/10.1103/PhysRevD.93.121301.

[26] Z. Pan and L. Knox. "Constraints on neutrino mass from cosmic microwave background and large-scale structure". In: *Monthly Notices of the Royal Astronomical Society* 454.3 (Oct. 2015), 3200–3206. ISSN: 1365-2966. DOI: 10.1093/mnras/stv2164. URL: http://dx.doi.org/10.1093/mnras/stv2164.

[27] Planck Collaboration. "Planck 2018 results. VIII. Gravitational lensing". In: *arXiv e-prints* (July 2018). arXiv: 1807.06210 [astro-ph.CO].

[28] Geraint Pratten and Antony Lewis. "Impact of post-Born lensing on the CMB". In: *Journal of Cosmology and Astroparticle Physics* 2016.08 (Aug. 2016), 047–047. ISSN: 1475-7516. DOI: 10.1088/1475-7516/2016/08/047. URL: http://dx.doi.org/10.1088/1475-7516/2016/08/047.

[29] Kendrick M Smith et al. "Delensing CMB polarization with external datasets". In: *Journal of Cosmology and Astroparticle Physics* 2012.06 (June 2012), pp. 014–014. ISSN: 1475-7516. DOI: 10.1088/1475-7516/2012/06/014. URL: http://dx.doi.org/10.1088/1475-7516/2012/06/014.

[30] M. Takada and B. Jain. "Cosmological parameters from lensing power spectrum and bispectrum tomography". In: *Monthly Notices of the Royal Astronomical Society* 340 (2003), pp. 580–608.

[31] Max Tegmark. "Cosmic Confusion: Degeneracies among Cosmological Parameters Derived from Measurements of Microwave Background Anisotropies". In: *Monthly Notices of the Royal Astronomical Society* 294.2 (1997), pp. 337–348. DOI: 10.1093/mnras/294.2.337.

[32] L. Van Waerbeke, Y. Mellier, T. Erben, et al. "Detection of correlated galaxy ellipticities from CFH12k VLT data: first evidence for gravitational lensing by large-scale structures". In: *Astronomy & Astrophysics* 358 (2000), pp. 30–44.

[33] L. van Waerbeke et al. "Measurement of cosmic shear three-point correlations in the VIRMOS-Descart survey". In: *Astronomy and Astrophysics* 393 (2002), pp. 369–381. arXiv: astro-ph/0101511 [astro-ph].

A Weak Lensing

A.1 Perturbed Photon Paths

We work in the conformal Newtonian gauge and with natural units. Denoting conformal time and conformal radial distance by η and χ, respectively, the perturbed line element in FLRW spacetime is given by

$$\mathrm{d}s^2 = a^2(\eta)((1+2\Psi_N)\mathrm{d}\eta^2 - (1+2\Phi_N)\gamma_{ij}\mathrm{d}x^i\mathrm{d}x^j), \tag{A.1}$$

where γ_{ij} is the unperturbed line element

$$\gamma_{ij} = \mathrm{d}x^i\mathrm{d}x^j = \mathrm{d}\chi^2 + f_K^2(\chi)(\mathrm{d}\theta^2 + \sin^2\theta\mathrm{d}\phi^2), \tag{A.2}$$

and $f_K(\chi)$ is the comoving angular diameter distance. We will hereafter only consider a flat universe so that $f_K(\chi) = \chi$. Weak lensing of a point source can be quantified by looking at the deflection field $\mathbf{d}(\hat{\mathbf{n}}) = \theta_{\mathrm{obs}} - \theta_{\mathrm{true}}$, i.e. the (small) difference between the angle at which we see the object

and the angle at which we would see the object had no lensing occurred. To first order in Ψ_N and Φ_N, the deflection is given as [12]

$$\mathbf{d}(\hat{\mathbf{n}}) = -2\int_0^{\chi_*} \mathrm{d}\chi \frac{\chi_* - \chi}{\chi_*\chi} \nabla_{\hat{\mathbf{n}}} \Psi(\chi\hat{\mathbf{n}}; \eta_0 - \chi), \tag{A.3}$$

where Ψ is the Weyl Potential, $\Psi := (\Psi_N - \Phi_N)/2$, and χ_* is the conformal distance to the source. $\nabla_{\hat{\mathbf{n}}}$ is the derivative along the axes orthogonal to the line of sight. The above equation can be written in terms of the lensing potential, ψ, as $\mathbf{d}(\hat{\mathbf{n}}) = \nabla_{\hat{\mathbf{n}}}\psi(\hat{\mathbf{n}})$, with

$$\psi(\hat{\mathbf{n}}) := -2\int_0^{\chi_*} \mathrm{d}\chi \frac{\chi_* - \chi}{\chi_*\chi} \Psi(\chi\hat{\mathbf{n}}; \eta_0 - \chi). \tag{A.4}$$

If the source is instead distributed over radial distance according to some distribution function $p(\chi)$, with $p(\chi)$ normalized to integrate to 1, the $(\chi_* - \chi)/(\chi_*\chi)$ factor is changed as

$$\frac{\chi_* - \chi}{\chi_*\chi} \to W(\chi) := \int_\chi^\infty \mathrm{d}\chi' p(\chi') \frac{\chi' - \chi}{\chi'\chi}.$$

$W(\chi)$ is then called the window function. In the most general case, the lensing potential is thus given by

$$\psi(\hat{\mathbf{n}}) := -2\int_0^\infty \mathrm{d}\chi W(\chi) \Psi(\chi\hat{\mathbf{n}}; \eta_0 - \chi). \tag{A.5}$$

The integration limit is sometimes also taken to be the surface of the last scattering, as any window function vanishes after that distance. In the case of CMB lensing we can take $p(\chi') = \delta(\chi' - \chi_*)$, in which case the window function reduces to $H(\chi_* - \chi)(\chi_* - \chi)/(\chi_*\chi)$, with $H(\chi)$ the Heaviside step function.

A.2 Convergence and Shear

The magnification matrix is defined as

$$A_{ij} := \delta_{ij} + \frac{\partial}{\partial n_j} d_i(\hat{\mathbf{n}}). \tag{A.6}$$

This matrix can be decomposed in the following form, which immediately gives us definitions for the **convergence**, κ, **shear**, γ_1 and γ_2, and **rotation**, ω:

$$A_{ij}(\hat{\mathbf{n}}) = \begin{pmatrix} 1 - \kappa - \gamma_1 & -\gamma_2 + \omega \\ -\gamma_2 - \omega & 1 - \kappa + \gamma_1 \end{pmatrix}. \tag{A.7}$$

At 1st order, A is a symmetric matrix by definition and ω vanishes, we will ignore it from here on out. Intuitively, A tells you how a small patch in the sky transforms due to lensing. If we change the unlensed direction of a light source by $\delta\hat{\mathbf{n}}$, then the corresponding change in direction in the lensed image can be calculated as

$$\hat{\mathbf{n}} + \delta\hat{\mathbf{n}} \to \hat{\mathbf{n}} + \delta\hat{\mathbf{n}} + \mathbf{d}(\hat{\mathbf{n}} + \delta\hat{\mathbf{n}}) = \hat{\mathbf{n}} + \mathbf{d}(\hat{\mathbf{n}}) + \delta\hat{\mathbf{n}} + A_{ij}(\delta\hat{\mathbf{n}})_j. \tag{A.8}$$

For an image of the sky, A_{ij} thus introduces distortion. Note that $|A_{ij}| = (1-\kappa)^2 + \omega^2 - |\gamma|^2 = 1 - 2\kappa + O(\kappa^2, \gamma^2, \omega^2)$. We can thus interpret κ as telling us about the overall magnification of the

source. The γ_i represents the area-preserving distortion, i.e. stretching and squeezing in a specific direction.

We can relate κ and γ directly to the lensing potential as

$$\kappa = \frac{1}{2}\nabla^2\psi, \quad \gamma_1 = \frac{1}{2}(\partial_{n_1}^2 - \partial_{n_2}^2)\psi, \quad \gamma_2 = \partial_{n_1}\partial_{n_2}\psi. \tag{A.9}$$

It is shown in appendix D that

$$\gamma := \gamma_1 + i\gamma_2 = \frac{1}{2}\eth_1(\eth_0\psi) \tag{A.10}$$

where the spin raising operator, $\eth_s$ acts on a spin s function defined on S^2 to create a spin $s+1$ function. $\eth_s$ can be written in spherical coordinates (θ, ϕ) as[3]

$$\eth_s = -\sin^s\theta(\partial_\theta + \frac{i}{\sin\theta})\frac{1}{\sin^s\theta}. \tag{A.11}$$

In this context, a spin s function refers to a function ${}_sf(\theta, \phi)$ that transforms under any rotation of coordinates by picking up a phase factor $e^{is\alpha}$, with α the angle of the rotation, i.e.

$$f'(\theta', \phi') = e^{is\alpha}f(\theta, \phi). \tag{A.12}$$

Shear is thus a spin 2 function, which can be checked by noting that rotating a galaxy image stretched and squeezed through weak lensing by 180 degrees gives the same stretching and squeezing, i.e. the same shear.

The spherical harmonics are eigenfunctions of ∇^2 and the spin raising and lowering operators. Using this property, the corresponding relations in spherical harmonic space can be shown to be

$$\kappa_{lm} = \frac{l(l+1)}{2}\psi_{lm}, \quad \gamma_{lm} = \frac{\sqrt{(l-1)l(l+1)(l+2)}}{2}\psi_{lm}.$$

B Weak Lensing Statistics

B.1 Lensing Potential Power spectrum

The lensing potential can be decomposed into spherical harmonics as

$$\psi(\hat{\mathbf{n}}) = \sum_{\ell m}\psi_{\ell m}Y_{\ell m}(\hat{\mathbf{n}}). \tag{B.1}$$

On the other hand, consider the decomposition of Ψ in Fourier modes with the Fourier convention $\Psi(\mathbf{x}, \eta) = \int \frac{\mathrm{d}^3\mathbf{k}}{(2\pi)^3}\Psi(\mathbf{k}, \eta)e^{i\mathbf{k}\cdot\mathbf{x}}$,

$$\psi(\hat{\mathbf{n}}) = -2\int_0^{\chi_*}\mathrm{d}\chi W(\chi)\int\frac{\mathrm{d}^3\mathbf{k}}{(2\pi)^3}\Psi(\mathbf{k}, \eta_0 - \chi)e^{i\mathbf{k}\cdot\hat{\mathbf{n}}\chi}. \tag{B.2}$$

[3] We use the physics convention for the definition of θ and ϕ here.

We can then relate the multipole modes of ψ to the Fourier modes of Ψ through

$$\psi_{lm} = \langle Y_\ell^m | \psi \rangle = \int \mathrm{d}^2\hat{\mathbf{n}} Y_\ell^m(\hat{\mathbf{n}})^* \psi(\hat{\mathbf{n}}) \tag{B.3}$$

$$= -2 \int \mathrm{d}^2\hat{\mathbf{n}} Y_l^m(\hat{\mathbf{n}})^* \int_0^{\chi_*} \mathrm{d}\chi W(\chi) \int \frac{\mathrm{d}^3\mathbf{k}}{(2\pi)^3} \Psi(\mathbf{k}, \eta_0 - \chi) e^{i\mathbf{k}\cdot\hat{\mathbf{n}}\chi} \tag{B.4}$$

Now define the power spectrum as

$$\langle \Psi(\mathbf{k}, \eta) \Psi(\mathbf{k}', \eta') \rangle = \frac{2\pi^2}{k^3} P_\Psi(k, \eta, \eta') \delta(\mathbf{k} + \mathbf{k}'), \tag{B.5}$$

with η denoting the conformal time. This gives

$$\langle \psi(\hat{\mathbf{n}}) \psi(\hat{\mathbf{n}}') \rangle = 4 \int_0^{\chi_*} \mathrm{d}\chi \int_0^{\chi_*} \mathrm{d}\chi' W(\chi) W(\chi') \int \frac{\mathrm{d}^3\mathbf{k}}{(2\pi)^6} \frac{2\pi^2}{k^3} P_\psi(k, \eta_0 - \chi, \eta_0 - \chi') e^{i\mathbf{k}\cdot\hat{\mathbf{n}}\chi} e^{-i\mathbf{k}\cdot\hat{\mathbf{n}}'\chi'}, \tag{B.6}$$

where we used that $\eta = \eta_0 - \chi$ along the unperturbed photon path (this is known as the Born approximation), with η_0 the time at which the light ray hits Earth. We can use the result

$$e^{i\mathbf{k}\cdot\hat{\mathbf{n}}\chi} = 4\pi \sum_{\ell m} i^\ell j_\ell(k\chi) Y_\ell^m(\hat{\mathbf{n}})^* Y_\ell^m(\hat{\mathbf{k}}) = 4\pi \sum_{\ell m} i^\ell j_\ell(k\chi) Y_\ell^m(\hat{\mathbf{n}}) Y_\ell^m(\hat{\mathbf{k}})^*, \tag{B.7}$$

where j_l is the spherical Bessel function, to rewrite the above equation. Using both versions of the identity above, we immediately get a factor $Y_\ell^m(\hat{\mathbf{k}}) Y_{\ell'}^{m'}(\hat{\mathbf{k}})^*$ in our integral. We can factor the differential element of $\mathrm{d}^3\mathbf{k}$ into a radial and angular part as $k^2 \mathrm{d}k \mathrm{d}^2\Omega_k$, with Ω_k the solid angle, to apply the orthonormality condition of the spherical harmonics. Note that we take the same sequence of steps a number of times in other parts of the derivations of the lensing spectra. We thus obtain

$$\langle \psi(\hat{\mathbf{n}}) \psi(\hat{\mathbf{n}}') \rangle = 4(4\pi)^2 \sum_{ll'mm'} i^{l-l'} \int_0^{\chi_*} \mathrm{d}\chi \int_0^{\chi_*} \mathrm{d}\chi' W(\chi) W(\chi') \tag{B.8}$$

$$\times \int \frac{k^2 \mathrm{d}k}{(2\pi)^6} \frac{2\pi^2}{k^3} j_\ell(k\chi) j_{\ell'}(k\chi') P_\psi(k, \eta_0 - \chi, \eta_0 - \chi') Y_{\ell m}(\hat{\mathbf{n}}) Y_{\ell' m'}(\hat{\mathbf{n}}')^* \delta_{\ell\ell'} \delta_{mm'}. \tag{B.9}$$

The angular power spectrum is defined similarly to the power spectrum, i.e.

$$\langle \psi_{\ell m} \psi^*_{\ell' m'} \rangle = \delta_{\ell\ell'} \delta_{mm'} C_\ell^\psi. \tag{B.10}$$

Note that the correlation is independent of m and m'. We can thus read from equation B.9 that

$$C_l^\psi = 4(4\pi)^2 \int_0^{\chi_*} \mathrm{d}\chi \int_0^{\chi_*} \mathrm{d}\chi' W(\chi) W(\chi') \int \frac{k^2 \mathrm{d}k}{(2\pi)^6} \frac{2\pi^2}{k^3} j_\ell(k\chi) j_\ell(k\chi') P_\psi(k, \eta_0 - \chi, \eta_0 - \chi'), \tag{B.11}$$

which can be simplified to

$$C_\ell^\psi = \frac{2}{\pi^2} \int_0^{\chi_*} \mathrm{d}\chi \int_0^{\chi_*} \mathrm{d}\chi' W(\chi) W(\chi') \int k^2 \mathrm{d}k j_\ell(k\chi) j_\ell(k\chi') \frac{P_\psi(k, \eta_0 - \chi, \eta_0 - \chi')}{k^3}. \tag{B.12}$$

To further evaluate the integral we will make the Limber approximation. The Bessel functions peak sharply at $l = x$[4], with the peak being increasingly sharp for higher l. Similarly to $\delta(x -$

[4]Some sources use $x \approx l + 1/2$ instead, which is slightly more accurate for larger scales (low l) and slightly less accurate for smaller scales.

$x_0)f(x) = \delta(x - x_0)f(x_0)$, we thus take $j_l(k\chi)f(k) \approx j_l(k\chi)f(l/\chi)$. The Bessel functions satisfy an orthogonality condition,

$$\int k^2 \mathrm{d}k j_\ell(k\chi) j_\ell(k\chi') = \frac{\pi}{2\chi^2}\delta(\chi - \chi'). \tag{B.13}$$

In combination with the Limber approximation we thus find

$$\int k^2 \mathrm{d}k j_\ell(k\chi) j_\ell(k\chi') f(k) \approx \frac{\pi}{2\chi^2}\delta(\chi - \chi') f(\ell/\chi). \tag{B.14}$$

It allows us to write the Limber-approximate angular spectrum as

$$C_\ell^\psi = \frac{2}{\pi^2}\int_0^{\chi_*} \mathrm{d}\chi \int_0^{\chi_*} \mathrm{d}\chi' W(\chi) W(\chi') \frac{\pi}{2\chi^2}\delta(\chi - \chi')\frac{\chi^3}{\ell^3} P_\psi(\ell/\chi, \eta_0 - \chi, \eta_0 - \chi') \tag{B.15}$$

$$= \frac{1}{\ell^3 \pi}\int_0^{\chi_*} \chi \mathrm{d}\chi W(\chi)^2 P_\psi(\ell/\chi, \eta_0 - \chi, \eta_0 - \chi). \tag{B.16}$$

B.2 Lensing potential bispectrum

The derivation of the bispectrum proceeds similarly to that of the power spectrum. We aim to compute the bispectrum of the lensing potential fields of 3 (possibly distinct sources), ψ_1, ψ_2, ψ_3.

$$\langle (\psi_1)_{\ell_1 m_1} (\psi_2)_{\ell_2 m_2} (\psi_3)_{\ell_3 m_3} \rangle = \prod_i \left(-2 \int \mathrm{d}^2\hat{\mathbf{n}}_i (Y_{\ell_i}^{m_i}(\hat{\mathbf{n}}_i))^* \int_0^{\chi_*} \mathrm{d}\chi_i W_i(\chi_i) \int \frac{\mathrm{d}^3\mathbf{k}_i}{(2\pi)^3} e^{i\mathbf{k}_i \cdot \hat{\mathbf{n}}_i \chi_i} \right)$$
$$\times \langle \prod_i \Psi(\mathbf{k}_i, \eta_0 - \chi_i) \rangle.$$

Defining the bispectrum of the gravitational potential as

$$\langle \prod_{i=1,2,3} \Psi(\mathbf{k}_i, \eta_0 - \chi_i) \rangle = (2\pi)^3 \delta(\mathbf{k}_1 + \mathbf{k}_2 + \mathbf{k}_3) B^\Psi(\{k_i\}, \{\eta_0 - \chi_i\}),$$

we rewrite the lensing potential bispectrum as

$$\langle (\psi_1)_{\ell_1 m_1} (\psi_2)_{\ell_2 m_2} (\psi_3)_{\ell_3 m_3} \rangle = \prod_i \left(-2 \int \mathrm{d}^2\hat{\mathbf{n}}_i (Y_{\ell_i}^{m_i}(\hat{\mathbf{n}}_i))^* \int_0^{\chi_*} \mathrm{d}\chi_i W_i(\chi_i) \int \frac{\mathrm{d}^3\mathbf{k}_i}{(2\pi)^3} e^{i\mathbf{k}_i \cdot \hat{\mathbf{n}}_i \chi_i} \right)$$
$$\times (2\pi)^3 \delta(\mathbf{k}_1 + \mathbf{k}_2 + \mathbf{k}_3) B^\Psi(\{k_i\}, \{\eta_0 - \chi_i\}).$$

Now using equation B.7 to rewrite the complex exponential:

$$\langle (\psi_1)_{\ell_1 m_1} (\psi_2)_{\ell_2 m_2} (\psi_3)_{\ell_3 m_3} \rangle$$
$$= \prod_i \left(-2 \int \mathrm{d}^2\hat{\mathbf{n}}_i (Y_{\ell_i}^{m_i}(\hat{\mathbf{n}}_i))^* \int_0^{\chi_*} \mathrm{d}\chi_i W_i(\chi_i) \int \frac{\mathrm{d}^3\mathbf{k}_i}{(2\pi)^3} 4\pi \sum_{\ell m} i^\ell j_l(k_i\chi_i) Y_\ell^m(\hat{\mathbf{n}}_i) Y_\ell^m(\hat{\mathbf{k}}_i)^* \right)$$
$$\times (2\pi)^3 \delta(\mathbf{k}_1 + \mathbf{k}_2 + \mathbf{k}_3) B^\Psi(\{k_i\}, \{\eta_0 - \chi_i\})$$
$$= \left[\prod_i \left(-2 \int_0^{\chi_*} \mathrm{d}\chi_i W_i(\chi_i) \int \frac{\mathrm{d}^3\mathbf{k}_i}{(2\pi)^3} 4\pi i^{\ell_i} j_{\ell_i}(k_i\chi_i) Y_{\ell_i}^{m_i}(\hat{\mathbf{k}}_i)^* \right) \right] (2\pi)^3 \delta(\mathbf{k}_1 + \mathbf{k}_2 + \mathbf{k}_3) B^\Psi(\{k_i\}, \{\eta_0 - \chi_i\}).$$

We can write the 3D Dirac delta function in terms of spherical harmonics as

$$\delta(\mathbf{k}_1+\mathbf{k}_2+\mathbf{k}_3) = 8\int \mathrm{d}^3\mathbf{x} \prod_{i=1,2,3}\left(\sum_{\ell_j m_j} i^{\ell_j} j_{\ell_j}(k_i x) Y_{\ell_j}^{m_j}(\hat{\mathbf{k}_i}) Y_{\ell_j}^{m_j}(\hat{\mathbf{x}})^*\right).$$

This results in

$$\langle(\psi_1)_{\ell_1 m_1}(\psi_2)_{\ell_2 m_2}(\psi_3)_{\ell_3 m_3}\rangle = \prod_i\left(-2\int_0^{\chi_*}\mathrm{d}\chi_i W_i(\chi_i)\int\frac{\mathrm{d}^3\mathbf{k}_i}{(2\pi)^3}4\pi i^{\ell_i} j_{\ell_i}(k_i\chi_i)Y_{\ell_i}^{m_i}(\hat{\mathbf{k}_i})^*\right)$$
$$\times(2\pi)^3 8\int\mathrm{d}^3\mathbf{x}\prod_i\left(\sum_{\ell m} i^{\ell} j_{\ell}(k_i x)Y_{\ell}^{m}(\hat{\mathbf{k}_i})Y_{\ell}^{m}(\hat{\mathbf{x}})^*\right)B^{\Psi}(\{k_i\},\{\eta_0-\chi_i\})$$
$$= (2\pi)^3 8\int\mathrm{d}^3\mathbf{x}\prod_i\left(-2\int_0^{\chi_*}\mathrm{d}\chi_i W_i(\chi_i)\int\frac{k_i^2\mathrm{d}k_i}{(2\pi)^3}4\pi(-1)^{\ell_i} j_{\ell_i}(k_i\chi_i)j_{\ell_i}(k_i x)Y_{\ell_i}^{m_i}(\hat{\mathbf{x}})^*\right)B^{\Psi}(\{k_i\},\{\eta_0-\chi_i\})$$

The angular part of the $\mathbf{x}$ integral can be evaluated using the identity

$$\int\mathrm{d}\Omega_{\hat{n}}\, Y^*_{\ell_1 m_1}(\hat{x})Y^*_{\ell_2 m_2}(\hat{n})Y^*_{\ell_3 m_3}(\hat{n}) = (-1)^{m_1+m_2+m_3}\int\mathrm{d}\Omega_{\hat{n}}\, Y_{\ell_1 -m_1}(\hat{n})Y_{\ell_2 -m_2}(\hat{n})Y_{\ell_3 -m_3}(\hat{n})$$
$$= (-1)^{m_1+m_2+m_3}\sqrt{\frac{(2\ell_1+1)(2\ell_2+1)(2\ell_3+1)}{4\pi}}\begin{pmatrix}\ell_1 & \ell_2 & \ell_3\\ 0 & 0 & 0\end{pmatrix}\begin{pmatrix}\ell_1 & \ell_2 & \ell_3\\ -m_1 & -m_2 & -m_3\end{pmatrix}\equiv A_{\mathrm{I}}^{\mathbf{m}},$$

giving

$$\langle(\psi_1)_{\ell_1 m_1}(\psi_2)_{\ell_2 m_2}(\psi_3)_{\ell_3 m_3}\rangle = (2\pi)^3 8A_{\mathrm{I}}^{\mathbf{m}}\int x^2\mathrm{d}x\prod_i\left(-2\int_0^{\chi_*}\mathrm{d}\chi_i W_i(\chi_i)\int\frac{k_i^2\mathrm{d}k_i}{(2\pi)^3}4\pi(-1)^{\ell_i} j_{\ell_i}(k_i\chi_i)j_{\ell_i}(k_i x)\right)$$
$$\times B^{\Psi}(\{k_i\},\{\eta_0-\chi_i\}).$$

Now applying the Limber approximation again:

$$\langle(\psi_1)_{\ell_1 m_1}(\psi_2)_{\ell_2 m_2}(\psi_3)_{\ell_3 m_3}\rangle = (2\pi)^3 8A_{\mathrm{I}}^{\mathbf{m}}\int x^2\mathrm{d}x\prod_i\left(-2\int_0^{\chi_*}\mathrm{d}\chi_i W_i(\chi_i)\frac{1}{(2\pi)^3}\frac{\pi}{2\chi_i^2}\delta(x-\chi_i)4\pi(-1)^{\ell_i}\right)$$
$$\times B^{\Psi}(\{\ell_i/\chi_i\},\{\eta_0-\chi_i\})$$
$$= (2\pi)^3 8A_{\mathrm{I}}^{\mathbf{m}}\int\chi^2\mathrm{d}\chi\prod_i\left(-2W_i(\chi)\frac{1}{(2\pi)^3}\frac{\pi}{2\chi^2}4\pi(-1)^{\ell_i}\right)B^{\Psi}(\{\ell_i/\chi\},\eta_0-\chi).$$

Finally, we aim to rewrite the above in terms of the angular bispectrum of the lensing potential.

The definition for the bispectrum of any set of randomly distributed spherical harmonic components $X_{\ell m}^k$ is [10]

$$\langle(X_1)_{\ell_1 m_1}(X_2)_{\ell_2 m_2}(X_3)_{x_3 m_3}\rangle = \begin{pmatrix}\ell_1 & \ell_2 & \ell_3\\ m_1 & m_2 & m_3\end{pmatrix}B_{\ell_1\ell_2\ell_3}^{X_1X_2X_3}.$$

Note the independence on m_i, this necessarily follows from statistical isotropy. If $m_1+m_2+m_3\neq 0$, the associated Wigner-3j symbol vanishes and the bispectrum is set to zero. Also note that in this definition we have immediately generalized to include cross correlation between different fields X_1, X_2, X_3. This is relevant when we look at cross-correlations between CMB and galaxy lensing. 6758 Using the above definition and the symmetry property

$$\begin{pmatrix}\ell_1 & \ell_2 & \ell_3\\ -m_1 & -m_2 & -m_3\end{pmatrix} = (-1)^{\ell_1+\ell_2+\ell_3}\begin{pmatrix}\ell_1 & \ell_2 & \ell_3\\ m_1 & m_2 & m_3\end{pmatrix},$$

we find

$$B^{\psi_1\psi_2\psi_3}_{\ell_1\ell_2\ell_3} = (-1)^{\ell_1+\ell_2+\ell_3}\sqrt{\frac{(2\ell_1+1)(2\ell_2+1)(2\ell_3+1)}{4\pi}}\begin{pmatrix}\ell_1 & \ell_2 & \ell_3\\ 0 & 0 & 0\end{pmatrix}(2\pi)^3 8$$
$$\times\int \chi^2 \mathrm{d}\chi \prod_i \left(-2W_i(\chi,\chi_*)\frac{1}{(2\pi)^3}\frac{\pi}{2\chi^2}4\pi(-1)^{\ell_i}\right) B^\Psi(\{\ell_i/\chi\},\{\eta_0-\chi\}),$$

where we were able to drop the $(-1)^{m_1+m_2+m_3}$ factor due to the bispectrum vanishing if that sum does not equal 0, as mentioned earlier. When all m_i equal zero, the Wigner 3j-symbol gains a number of useful properties In particular, it vanishes if $\ell_1+\ell_2+\ell_3$ is odd, meaning we can drop the $(-1)^{\ell_1+\ell_2+\ell_3}$ factor. Additionally cancelling common factors then gives

$$B^{\psi_1\psi_2\psi_3}_{\ell_1\ell_2\ell_3} = -\sqrt{\frac{(2\ell_1+1)(2\ell_2+1)(2\ell_3+1)}{4\pi}}\begin{pmatrix}\ell_1 & \ell_2 & \ell_3\\ 0 & 0 & 0\end{pmatrix}8\int\frac{\mathrm{d}\chi}{\chi^4}W_1(\chi)W_2(\chi)W_3(\chi)B^\Psi(\{l_i/\chi\},\eta_0-\chi). \tag{B.17}$$

B.3 Gravitational potential spectra in terms of matter spectra

We can rewrite equations B.16 and B.17 in terms of the matter spectra instead of the ψ spectra using the poisson equation. This allows us to numerically evaluate these lensing spectra using CAMB. The density contrast is defined as

$$\delta(\mathbf{x}) := \frac{\rho(\mathbf{x})-\bar\rho}{\bar\rho}, \tag{B.18}$$

and the matter spectra are defined in terms of the fourier transformed density contrast $\delta(\mathbf{k})$ as

$$\langle\delta(\mathbf{k},\eta)\delta(\mathbf{k}',\eta)^*\rangle = (2\pi)^3\delta(\mathbf{k}-\mathbf{k}')P^\delta(\mathbf{k},\eta),$$
$$\langle\delta(\mathbf{k}_1,\eta)\delta(\mathbf{k}_2,\eta)\delta(\mathbf{k}_3,\eta)\rangle = (2\pi)^3\delta(\mathbf{k}_1+\mathbf{k}_2+\mathbf{k}_3)B^\delta(k_1,k_2,k_3,\eta).$$

The mean matter density of the universe, $\bar\rho$ is given as

$$\bar\rho(\eta) = \frac{3\Omega_m H_0^2}{8\pi G}\frac{1}{a(\eta)^3},$$

where $a(\eta)$ is the only time dependent factor on the right hand side. The poisson equation relates Ψ to the density contrast as [12]

$$\nabla^2\Psi(\mathbf{x}) = 4\pi G a^2\left(\frac{3\Omega_m H_0^2}{8\pi G}\frac{1}{a^3}\right)\delta(\mathbf{x}) = \frac{3\Omega_m H_0^2}{2}\frac{1}{a}\delta(\mathbf{x}) \implies \Psi(k,\eta) = -\frac{3\Omega_m H_0^2}{2}\frac{1}{a}\frac{\delta(k,\eta)}{k^2}, \tag{B.19}$$

where $\Psi(k,\eta)$ and $\delta(k,\eta)$ are functions in Fourier space. For the power- and bispectra we find

$$\langle\Psi(\mathbf{k},\eta)\Psi^*(\mathbf{k}',\eta)\rangle = \frac{2\pi^2}{k^3}C^\Psi(k,\eta)\delta(\mathbf{k}-\mathbf{k}') \implies C^\Psi(k,\eta) = \frac{1}{k}(9\Omega_m^2 H_0^4\pi)\frac{1}{a^2}C^\delta(k,\eta),$$
$$\langle\Psi(\mathbf{k}_1,\eta)\Psi(\mathbf{k}_2,\eta)\Psi(\mathbf{k}_3,\eta)\rangle = -(2\pi)^3\delta(\mathbf{k}_1+\mathbf{k}_2+\mathbf{k}_3)B^\Psi(k_1,k_2,k_3,\eta)$$
$$\implies B^\Psi(k_1,k_2,k_3,\eta) = -\frac{1}{k_1^2k_2^2k_3^2}\left(\frac{3\Omega_m H_0^2}{2}\right)^3\frac{1}{a^3}B^\delta(\{k_i\},\eta).$$

Finally, we obtain:

$$\boxed{\begin{aligned} C_\ell^{\psi_X\psi_Y} &= \frac{9}{\ell^4}\Omega_m^2 H_0^4 \int_0^{\chi_*} \chi^2 \mathrm{d}\chi a(\eta_0-\chi)^{-2} W_X(\chi) W_Y(\chi) P^\delta(\ell/\chi, \eta_0-\chi), \\ B^{\psi_X\psi_Y\psi_Z}_{\ell_1\ell_2\ell_3} &= \sqrt{\frac{(2\ell_1+1)(2\ell_2+1)(2\ell_3+1)}{4\pi}} \begin{pmatrix} \ell_1 & \ell_2 & \ell_3 \\ 0 & 0 & 0 \end{pmatrix} \frac{27}{\ell_1^2\ell_2^2\ell_3^2}\Omega_m^3 H_0^6 \\ &\quad \times \int \chi^2 \mathrm{d}\chi a(\eta_0-\chi)^{-3} W_X(\chi) W_Y(\chi) W_Z(\chi) B^\delta(\{\ell_i/\chi\}, \eta_0-\chi). \end{aligned}}$$

C Fisher Matrix Analysis

C.1 Determing uncertainty in experimental parameters

The Fisher matrix formalism is used to find a lower bound on the constraints we can place on experimental parameters. It combines the Cramer-Rao Inequality [8] with the assumption that we have unbiased estimators following a gaussian distribution [12]. In particular, denoting the Fisher matrix by $F_{\theta_i\theta_j}$, the parameters as θ_i, and their estimators as $\hat{\theta}_i$, it can be shown that

$$\mathrm{Var}(\hat{\theta}_i) \geq \left(F^{-1}\right)_{\theta_i\theta_i}. \tag{C.1}$$

In the case of n measurements whose outcomes are realizations of random variables x_i, each with associated mean μ_{x_i}, the Fisher matrix is given as

$$F_{\theta_i\theta_j} := \sum_{p,q=1}^{n} \frac{\partial \mu_{x_p}}{\partial\theta_i}(\tilde{\theta}_k)(\mathrm{Cov}^{-1})_{x_p x_q}(\tilde{\theta}_k)\frac{\partial \mu_{x_q}}{\partial\theta_j}(\tilde{\theta}_k), \tag{C.2}$$

where Cov is the covariance matrix associated with the random vector $(x_1, ..., x_n)$, $\mathrm{Cov}_{x_p x_q} := \mathrm{Cov}(x_p, x_q)$. The derivative of the mean measurement outcomes and measurement covariances will in general depend on the true, unknown, values of the experimental parameters. We therefore evaluate these quantities with for our best guess of the experimental parameters given some outside information. These are known as the "fiducial" values.

C.2 Fisher matrices for power- and bispectra with multiple tracers

For power spectra, the definition of the Fisher matrix gives

$$F_{\alpha\beta} = \sum_{l_{min}\leq\ell,\ell'\leq\ell_{max}} \sum_{[XY][X'Y']} \partial_\alpha C_\ell^{XY} \left(\mathrm{Cov}^{-1}\right)_{\ell,\ell'}^{XY,X'Y'} \partial_\beta C_{\ell'}^{X'Y'}.$$

Here the covariance matrix is given as

$$\mathrm{Cov}_{\ell,\ell'}^{XY,X'Y'} = \langle \hat{C}_\ell^{XY} \hat{C}_{\ell'}^{X'Y'} \rangle.$$

The estimator of the power- or bi-spectrum is the product of the estimators of the appropriate tracers, e.g. $\hat{C}_\ell^{XY} = \hat{X}(\ell)\hat{Y}(\ell)$. The sum over $[XY]$ and $[X'Y']$ denotes a sum over possible tracer combinations *without* counting permutations of tracer configuration. This is because permutations

are not distinct signals, i.e. $\hat{X}(\ell)\hat{Y}(\ell) = \hat{Y}(\ell)\hat{X}(\ell)$. In fact, if we were to count these permutations as distinct signals we would get identical columns and/or rows in our covariance matrix making inversion impossible:

$$\langle \hat{X}(\ell)\hat{Y}(\ell)\hat{X}'(\ell')\hat{Y}'(\ell')\rangle = \langle \hat{Y}(\ell)\hat{X}(\ell)\hat{X}'(\ell')\hat{Y}'(\ell')\rangle, \quad \forall X', Y', \ell'.$$

To evaluate the covariance matrix we again assume that the estimators are Gaussian distributed so that we can apply a wick contraction, as is commonly done [31]. In this case we get

$$\mathrm{Cov}_{\ell,\ell'}^{XY,X'Y'} = \frac{1}{2\ell+1}\delta_{\ell\ell'}\left(\tilde{C}_\ell^{XX'}\tilde{C}_\ell^{YY'} + \tilde{C}_\ell^{XY'}\tilde{C}_\ell^{YX'}\right).$$

Two remarks are in order.

1. By definition
$$\langle X_{\ell m} X'_{\ell' m'}\rangle = (2\pi)^3\delta_{\ell\ell'}\delta_{mm'}C_\ell^{XX'},$$
so you can average over the measurements done for different values of m, i.e. $X_{\ell(-\ell)}$, $X_{\ell(-\ell+1)}$, $\cdots$, $X_{\ell(\ell-1)}$, $X_{\ell\ell}$. This results in the $(2\ell+1)^{-1}$ factor in the power spectrum covariance.

2. The tilde is used to denote the power spectrum as calculated earlier plus the noise power spectrum, $N_\ell^{XX'}$, which is the power spectrum of the noise associated with the estimator of the field. This is where experimental noise is incorporated into the calculation.

Under the Gaussian approximation, the covariance matrix vanishes except for 3×3 block matrices (in the case of 2 tracers) on the diagonal. The fisher matrix is then

$$F_{\alpha\beta} = \sum_\ell \sum_{[XY][X'Y']} \partial_\alpha C_\ell^{XY}\left(\mathrm{Cov}_\ell^{-1}\right)^{XY,X'Y'}\partial_\beta C_\ell^{X'Y'}.$$

Cov_ℓ^{-1} here denotes the inverse of the block matrix at l.

Next, we consider the Fisher matrix for bispectra measurements.

$$F_{\alpha\beta} = \sum_{\text{distinct signals}} \sum_{\text{distinct signals prime}} B_{\ell_1\ell_2\ell_3}^{XYZ}\left(\mathrm{Cov}^{-1}\right)_{\ell_1\ell_2\ell_3,\ell_1'\ell_2'\ell_3'}^{XYZ,X'Z'Y'} B_{\ell_1'\ell_2'\ell_3'}^{X'Y'Z'}.$$

Counting only distinct signals requires more care compared to the power spectra. The rule is that $B_{\ell_1\ell_2\ell_3}^{XYZ}$ and $B_{\ell_1'\ell_2'\ell_3'}^{X'Y'Z'}$ are not distinct signals if there exists a permutation σ that simultaniously maps $X'Y'Z'$ to XYZ and $\ell_1'\ell_2'\ell_3'$ to $\ell_1\ell_2\ell_3$. It turns out that we can write a sum over distinct signals explicitly as

$$\sum_{\text{distinct signals}} = \underbrace{\sum_{\ell_1=\ell_2=\ell_3}\sum_{[XYZ]}}_{\text{sum 1}} + \underbrace{\sum_{\ell_1=\ell_2\neq\ell_3}\sum_{[XY]Z}}_{\text{sum 2}} + \underbrace{\sum_{\ell_1<\ell_2<\ell_3}\sum_{XYZ}}_{\text{sum 3}}.$$

With the same definition again for the $[\cdot]$ notation. For example:

$$\{[XY]Z|X,Y,Z\in\{\psi_\kappa,\psi_\gamma\}\} = \{\psi_\kappa\psi_\kappa\psi_\kappa, \psi_\kappa\psi_\gamma\psi_\kappa, \psi_\gamma\psi_\gamma\psi_\kappa, \psi_\kappa\psi_\kappa\psi_\gamma, \psi_\kappa\psi_\gamma\psi_\gamma, \psi_\gamma\psi_\gamma\psi_\gamma\}.$$

It follows to show that the sets that these sums sum over form a partition of the set of all distinct signals. Clearly all 3 sets are pairwise disjoint (no common elements) because of the criteria for the l_i's. To show that their union covers the set of distinct signals, start by considering an arbitrary signal. Its l configuration will trivially correspond to exactly one of the three sums. If it is sum 1, then we are free to permute the XYZ's by virtue of the l's being identical so we will be able to match the XYZ configuration to one of the elements of $\{\{XYZ\}\}$. Similarly, if the l configuration corresponds to sum 2, then we are free to permute the XY configuration to match with one of the elements of $\{\{XY\}Z\}$. The Z value does not matter because any Z value is accounted for. For sum 3 we can argue that we can switch around the order of the l's to satisfy $\ell_1 < l2 < l3$ and the corresponding XYZ configuration will be accounted for in sum 3 because all XYZ combinations are counted. Finally, it is simple to verify that no distinct signal is counted more than once within each sum.

To calculate the elements of the covariance matrix consider the following. Every element of the Fisher matrix can be seen as an inner product weighted by the inverse covariance matrix. We can choose how we order the vectors[5]. We organize the vectors according to the sum 1, 2, and 3 parts first. Then by l configuration. Within each l configuration we can choose any ordering for the XYZ configurations. The covariance matrix now becomes a block matrix with each block corresponding to an l_i and l_i' configuration. When wick contracting using the gaussian approximation, every block matrix where $(\ell_1, \ell_2, \ell_3) \neq (\ell_1', \ell_2', \ell_3')$ vanishes. It can then be shown that the entries of each block matrix are given as

$$\begin{aligned}(\mathrm{Cov}_{\ell_1\ell_2\ell_3})^{XYZ,X'Y'Z'} &= \tilde{C}_{\ell_1}^{XX'}\tilde{C}_{\ell_2}^{YY'}\tilde{C}_{\ell_3}^{ZZ'} + \delta_{\ell_1\ell_2}\tilde{C}_{\ell_1}^{XY'}\tilde{C}_{\ell_2}^{YX'}\tilde{C}_{\ell_3}^{ZZ'} + \delta_{\ell_2\ell_3}\tilde{C}_{\ell_1}^{XX'}\tilde{C}_{\ell_2}^{YZ'}\tilde{C}_{\ell_3}^{ZX'} \\ &+\delta_{\ell_3\ell_1}\tilde{C}_{\ell_1}^{XZ'}\tilde{C}_{\ell_2}^{YY'}\tilde{C}_{\ell_3}^{ZX'} + \delta_{\ell_1\ell_2}\delta_{\ell_2\ell_3}\left(\tilde{C}_{\ell_1}^{XY'}\tilde{C}_{\ell_2}^{YZ'}\tilde{C}_{\ell_3}^{ZX'} + \tilde{C}_{\ell_1}^{XZ'}\tilde{C}_{\ell_2}^{YX'}\tilde{C}_{\ell_3}^{ZY'}\right).\end{aligned}$$

With our ordering this means that the covariance matrix is again a diagonal block matrix, now with blocks of size 4×4 (sum 1), 6×6 (sum 2), and 8×8 (sum 3).

C.3 Explicit form for inverse covariance matrix

The Fisher matrix above can be significantly simplified and written as

$$F_{\alpha\beta} = \sum_{\ell_1 \leq \ell_2 \leq \ell_3} \frac{\mathcal{P}_{\ell_1\ell_2\ell_3}}{6} \sum_{XYZ} \sum_{X'Y'Z'} \partial_\alpha B_{\ell_1\ell_2\ell_3}^{XYZ} (\tilde{C}^{-1})_{\ell_1}^{XX'} (\tilde{C}^{-1})_{\ell_2}^{YY'} (\tilde{C}^{-1})_{\ell_3}^{ZZ'} \partial_\beta B_{\ell_1\ell_2\ell_3}^{X'Y'Z'}$$

where, in the case of two tracers,

$$C_l := \begin{pmatrix} \tilde{C}_l^{\psi_1\psi_1} & \tilde{C}_l^{\psi_1\psi_2} \\ \tilde{C}_l^{\psi_1\psi_2} & \tilde{C}_l^{\psi_2\psi_2} \end{pmatrix}$$

and $\mathcal{P}_{\ell_1\ell_2\ell_3}$ is defined as the number of distinct permutations that can be made with $\ell_1\ell_2\ell_3$. This form was, for example, used in [19][6].

[5] The entries are the derivatives of the bispectra

[6] Note that in [19] this is based on a previous equation summing over *all* l_i (so including permutations of each configuration) which is missing a factor of 1/6.

To show that the above is the same as the formula for the Fisher matrix given earlier, first parition the sum in the same way and collect all terms that fit in the different categories.

$$
\begin{aligned}
F_{\alpha\beta} = &\sum_{\ell_1=\ell_2=\ell_3} \sum_{[XYZ]} \sum_{[X'Y'Z']} \partial_\alpha B^{XYZ}_{\ell_1\ell_2\ell_3} \left(\frac{\mathcal{P}_{\ell_1\ell_2\ell_3}}{6} \sum_{d.p.XYZ} \sum_{d.p.X'Y'Z'} (\tilde{C}^{-1})^{XX'}_{\ell_1} (\tilde{C}^{-1})^{YY'}_{\ell_2} (\tilde{C}^{-1})^{ZZ'}_{\ell_3} \right) \partial_\beta B^{X'Y'Z'}_{\ell_1\ell_2\ell_3} \\
&+ \sum_{\ell_1=\ell_2\neq\ell_3} \sum_{[XY]Z} \sum_{[X'Y']Z'} \partial_\alpha B^{XYZ}_{\ell_1\ell_2\ell_3} \left(\frac{\mathcal{P}_{\ell_1\ell_2\ell_3}}{6} \sum_{d.p.XY} \sum_{d.p.X'Y'} (\tilde{C}^{-1})^{XX'}_{\ell_1} (\tilde{C}^{-1})^{YY'}_{\ell_2} (\tilde{C}^{-1})^{ZZ'}_{\ell_3} \right) \partial_\beta B^{X'Y'Z'}_{\ell_1\ell_2\ell_3} \\
&+ \sum_{\ell_1<\ell_2<\ell_3} \sum_{XYZ} \sum_{X'Y'Z'} \partial_\alpha B^{XYZ}_{\ell_1\ell_2\ell_3} (\tilde{C}^{-1})^{XX'}_{\ell_1} (\tilde{C}^{-1})^{YY'}_{\ell_2} (\tilde{C}^{-1})^{ZZ'}_{\ell_3} \partial_\beta B^{X'Y'Z'}_{\ell_1\ell_2\ell_3},
\end{aligned}
$$

where "*d.p.*" stands for "distinct permutations". The entries above are then the entries of the inverses of the block matrices mentioned earlier. This can be checked. For example, for the $\ell_1 = \ell_2 = \ell_3$ sum the multiplication of block matrices corresponding to the same l_i configuration can be written as:

$$
\begin{aligned}
&\sum_{[X'Y'Z']} \left(\frac{\mathcal{P}_{\ell_1\ell_2\ell_3}}{6} \sum_{d.p.XYZ} \sum_{d.p.X'Y'Z'} (\tilde{C}^{-1})^{XX'}_{l} (\tilde{C}^{-1})^{YY'}_{l} (\tilde{C}^{-1})^{ZZ'}_{l} \right) \left(\tilde{C}^{X'X''}_{l} \tilde{C}^{Y'Y''}_{l} \tilde{C}^{Z'Z''}_{l} + \text{perms } X''Y''Z'' \right) \\
&= \frac{\mathcal{P}_{\ell_1\ell_2\ell_3}}{6} \left[\left(\sum_{d.p.XYZ} \sum_{X'Y'Z'} (\tilde{C}^{-1})^{XX'}_{l} (\tilde{C}^{-1})^{YY'}_{l} (\tilde{C}^{-1})^{ZZ'}_{l} \right) \tilde{C}^{X'X''}_{l} \tilde{C}^{Y'Y''}_{l} \tilde{C}^{Z'Z''}_{l} \right] + \text{perms } X''Y''Z'' \\
&= \frac{\mathcal{P}_{\ell_1\ell_2\ell_3}}{6} \sum_{d.p.XYZ} \delta_{XX''}\delta_{YY''}\delta_{ZZ''} + \text{perms } X''Y''Z'' = \frac{\mathcal{P}_{\ell_1\ell_2\ell_3}}{6} \delta_{[XYZ],[X''Y''Z'']} + \text{perms } X''Y''Z'' \\
&= \delta_{[XYZ],[X''Y''Z'']}.
\end{aligned}
$$

The sum over the different wick contractions will similarly cancel with the $\mathcal{P}_{\ell_1\ell_2\ell_3}/6$ factor for the $\ell_1 = \ell_2 \neq \ell_3$ sum. For the $\ell_1 < \ell_2 < \ell_3$ sum the proof is similar as well except no cancellation is required.

The same type of simplification can be made in the Fisher matrix for the power spectrum, though it doesn't offer any significant benefits compared to our current 3×3 block matrix form.

C.4 Signal to Noise Ratio (SNR)

To quantify the detectability of the lensing spectra, we introduce an overal amplitude of our signal, A, with fiducial value 1 as experimental parameter and compute F_{AA}. Obviously, $\partial_A \left(A B^{XYZ}_{\ell_1\ell_2\ell_3} \right)|_{A=1} = B^{XYZ}_{\ell_1\ell_2\ell_3}$, so we find

$$
\left(\frac{S}{N} \right)^2 := F_{AA} = \sum_{XYZ,X'Y'Z'} \sum_{\ell_1\leq\ell_2\leq\ell_3} \frac{\mathcal{P}_{\ell_1\ell_2\ell_3}}{6} B^{XYZ}_{\ell_1\ell_2\ell_3} (\tilde{C}^{-1})^{XX'}_{\ell_1} (\tilde{C}^{-1})^{YY'}_{\ell_2} (\tilde{C}^{-1})^{ZZ'}_{\ell_3} B^{X'Y'Z'}_{\ell_1\ell_2\ell_3}.
$$

The equation for the SNR of the power spectra is identical in form.

C.5 Fisher matrix of power- + bispectra

To compute the Fisher matrix of an experiment measuring both lensing power- and bispectra we are required to compute and invert the full covariance matrix. If we keep assuming that the measurements are close enough to Gaussian to be able to use wick contractions to a good approximation, the full covariance matrix simplifies trivially. The correlation between a power- and bispectrum estimator contains an odd (5) amount of fields and thus always vanishes. We are thus allowed to simply add the Fisher matrices of the power- and bispectra to compute the combined Fisher matrix.

D Shear equals twice spin raised lensing potential

Consider a point on S^2, (r_0, θ_0, ϕ_0), at which we observe some cosmological object. We can then define a set of cartesian coordinates $(\tilde{r}, \tilde{y}, \tilde{x})$ as shown in figure 7.

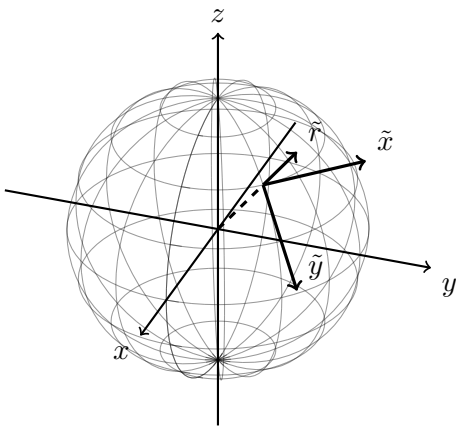

Figure 7. $(\tilde{r}, \tilde{y}, \tilde{x})$ coordinates defined for a point on the unit sphere. These act as ordinary cartesian coordinates but rotated such that, at the associated point on S^2, $\hat{\tilde{r}}$ points straight out of the unit sphere, $\hat{\tilde{y}}$ is parallel to the great arc with constant ϕ and $\hat{\tilde{x}}$ is parallel to the great arc with constant θ. These coordinates are used to define the shear and convergence in terms of the lensing potential.

Note that it is not obvious whether to define these coordinates at the point where the lensed light hits S^2 or the unlensed light hits S^2. We will assume that lensing effects are sufficiently weak that either definition works. We can then express the tilde coordinates in terms of spherical coordinates either by applying a rotation matrix or by calculating the r, θ, ϕ derivatives of (x, y, z) coordinates at (r_0, θ_0, ϕ_0) to find $\hat{\tilde{\mathbf{r}}}$, $\hat{\tilde{\boldsymbol{\theta}}}$, and $\hat{\tilde{\boldsymbol{\phi}}}$ and then take inner products. Regardless, we find

$$\tilde{r} = r\sin\theta\cos\phi\sin\theta_0\cos\phi_0 + r\sin\theta\sin\phi\sin\theta_0\sin\phi_0 + r\cos\theta\cos\theta_0, \tag{D.1}$$

$$\tilde{y} = r\sin\theta\cos\phi\cos\theta_0\cos\phi_0 + r\sin\theta\sin\phi\cos\theta_0\sin\phi_0 - r\cos\theta\sin\theta_0, \tag{D.2}$$

$$\tilde{x} = -r\sin\theta\cos\phi\sin\phi_0 + r\sin\theta\sin\phi\cos\phi_0. \tag{D.3}$$

This gives derivatives

$$\begin{aligned}\frac{\partial}{\partial\theta} =& (r\cos\theta\cos\phi\sin\theta_0\cos\phi_0 + r\cos\theta\sin\phi\sin\theta_0\sin\phi_0 - r\sin\theta\cos\theta_0)\,\frac{\partial}{\partial\tilde{r}}\\ &+ (r\cos\theta\cos\phi\cos\theta_0\cos\phi_0 + r\cos\theta\sin\phi\cos\theta_0\sin\phi_0 + r\sin\theta\sin\theta_0)\,\frac{\partial}{\partial\tilde{y}}\\ &+ (-r\cos\theta\cos\phi\sin\phi_0 + r\cos\theta\sin\phi\cos\phi_0)\,\frac{\partial}{\partial\tilde{x}}.\\ \frac{\partial}{\partial\phi} =& (-r\sin\theta\sin\phi\sin\theta_0\cos\phi_0 + r\sin\theta\cos\phi\sin\theta_0\sin\phi_0)\,\frac{\partial}{\partial\tilde{r}}\\ &+ (-r\sin\theta\sin\phi\cos\theta_0\cos\phi_0 + r\sin\theta\cos\phi\cos\theta_0\sin\phi_0)\,\frac{\partial}{\partial\tilde{y}}\\ &+ (r\sin\theta\sin\phi\sin\phi_0 + r\sin\theta\cos\phi\cos\phi_0)\,\frac{\partial}{\partial\tilde{x}}.\end{aligned}$$

Evaluated at our point of interest we obtain $\partial_\theta = \partial_{\tilde{y}}$ and $\partial_\phi = \sin\theta_0\partial_{\tilde{x}}$. The second-order derivatives can then be obtained using the first-order derivatives. We can immediately evaluate them at the point to get

$$\begin{aligned}\partial^2_\phi|_{(r_0,\theta_0,\phi_0)} &= -\sin^2\theta_0\partial_{\tilde{r}} - \sin\theta_0\cos\theta_0\partial_{\tilde{y}} + \sin^2\theta_0\partial^2_{\tilde{x}},\\ \partial_\theta\partial_\phi|_{(r_0,\theta_0,\phi_0)} &= \cos\theta_0\partial_{\tilde{x}} + \sin\theta_0\partial_{\tilde{x}}\partial_{\tilde{y}},\\ \partial^2_\theta|_{(r_0,\theta_0,\phi_0)} &= -\partial_{\tilde{r}} + \partial^2_{\tilde{y}}.\end{aligned}$$

Thus, at (r_0, θ_0, ϕ_0),

$$\begin{aligned}\frac{1}{2}\eth_1(\eth_0\psi) &= \frac{1}{2}\sin\theta(\partial_\theta + \frac{i}{\sin\theta}\partial_\phi)(\frac{1}{\sin\theta}(\partial_\theta + \frac{1}{\sin\theta}\partial_\phi))\\ &= \frac{\partial^2\psi}{\partial\theta^2} - \frac{\cos\theta}{\sin\theta}\frac{\partial\psi}{\partial\theta} + \frac{2i}{\sin\theta}\frac{\partial^2\psi}{\partial\theta\partial\phi} - \frac{1}{\sin^2\theta}\frac{\partial^2\psi}{\partial\phi^2} - 2i\frac{\cos\theta}{\sin^2\theta}\frac{\partial\psi}{\partial\phi}\\ &= \frac{1}{2}(\partial^2_{\tilde{y}} - \partial^2_{\tilde{x}} + 2i\partial_{\tilde{x}}\partial_{\tilde{y}})\psi = \gamma_1 + i\gamma_2 = \gamma.\end{aligned}$$

E Numerical derivative

The derivatives with respect to cosmological parameters were taken with a central difference formula, i.e.

$$f'(x) = \frac{f(x+h) - f(x-h)}{2h} + \mathcal{O}(h^2).$$

Each change of the cosmological parameters requires a recalculation of the entire cosmology, making it computationally expensive. For the approximation to be accurate a balance needs to be found between numerical errors for small h and a larger $\mathcal{O}(h^2)$ error for larger h. The h values chosen for each parameter are shown in table 4 and are similar to the values used in [25][7].

To test the accuracy, we varied h by $\pm5\%$ and $\pm10\%$ and compared the relative change in the derivative of the equilateral lensing bispectra and the lensing powerspectra. As long as numerical

[7] As confirmed during a conversation with the author.

Parameter	Fiducial value	Finite difference (h)
H	67.4	fiducial $\times 0.1$
$\Omega_b h^2$	0.0223	fiducial $\times 0.1$
$\Omega_c h^2$	0.119	fiducial $\times 0.005$
n_s	0.965	fiducial $\times 0.005$
A_s	2.13×10^{-9}	fiducial $\times 0.1$
τ	0.063	fiducial $\times 0.1$
m_ν	0.06	fiducial $\times 0.1$
w_0	-1	0.03

Table 4. Fiducial cosmological parameters and their finite-difference steps

noise doesn't dominate, it can be shown that the relative error in our approximation is approximately 5 times the relative difference that taking $h \to h(1 \pm 0.1)$ leads to. We thus conclude that, based on the tests conducted, the derivatives are almost always computed with up to one percent error. The exception is the derivative with respect to neutrino masses, which introduces a larger error of around 10 percent.

F ΛCDM constraints

We do not expect to use weak lensing surveys to competitively constrain the main ΛCDM parameters. Despite this, we include these constraints for completeness in figures 8 and 9 for CMB and galaxy lensing, respectively, and in table 5. CMB and galaxy lensing respectively. All survey parameters are the same as in section 4.

weak priors										
		CMB lensing			Gal. lensing			CMB × Gal. lensing		
Par	prior	C_ℓ	$B_{\ell_1\ell_2\ell_3}$	$C_\ell + B_{\ell_1\ell_2\ell_3}$	C_ℓ	$B_{\ell_1\ell_2\ell_3}$	$C_\ell + B_{\ell_1\ell_2\ell_3}$	C_ℓ	$B_{\ell_1\ell_2\ell_3}$	$C_\ell + B_{\ell_1\ell_2\ell_3}$
H_0	1.73e+01	1.65e+01	1.65e+01	6.91e+00	6.39e+00	5.04e+00	1.65e+00	4.13e+00	2.88e+00	6.65e-01
$\Omega_b h^2$	5.00e-04	5.00e-04	5.00e-04	5.00e-04	5.00e-04	4.98e-04	4.95e-04	4.86e-04	4.94e-04	4.65e-04
$\Omega_c h^2$	2.89e-01	6.99e-03	1.35e-02	6.42e-03	5.22e-03	4.74e-03	2.04e-03	1.07e-03	2.63e-03	8.62e-04
n_s	2.00e-02	1.90e-02	1.99e-02	1.82e-02	8.04e-03	1.89e-02	5.54e-03	2.98e-03	1.52e-02	2.34e-03
τ	6.30e-02	4.69e-04	6.30e-02	4.46e-04	6.30e-02	6.30e-02	6.30e-02	5.20e-05	6.30e-02	5.07e-05
A_s	1.00e-09	3.64e-10	9.29e-10	3.07e-10	2.56e-10	1.16e-10	7.27e-11	8.39e-11	1.10e-10	4.51e-11
CMB $T + E$ priors										
		CMB lensing			Gal. lensing			CMB × Gal. lensing		
Par	prior	C_ℓ	$B_{\ell_1\ell_2\ell_3}$	$C_\ell + B_{\ell_1\ell_2\ell_3}$	C_ℓ	$B_{\ell_1\ell_2\ell_3}$	$C_\ell + B_{\ell_1\ell_2\ell_3}$	C_ℓ	$B_{\ell_1\ell_2\ell_3}$	$C_\ell + B_{\ell_1\ell_2\ell_3}$
H_0	1.21e+00	1.00e+00	1.18e+00	1.00e+00	1.07e+00	9.93e-01	7.20e-01	9.32e-01	9.68e-01	5.17e-01
$\Omega_b h^2$	5.69e-05	5.16e-05	5.67e-05	5.15e-05	5.49e-05	5.29e-05	5.18e-05	4.74e-05	5.15e-05	4.69e-05
$\Omega_c h^2$	8.27e-04	6.08e-04	8.15e-04	5.99e-04	5.89e-04	6.57e-04	5.27e-04	1.63e-04	6.03e-04	1.54e-04
n_s	2.50e-03	2.17e-03	2.50e-03	2.15e-03	2.12e-03	2.42e-03	2.11e-03	1.44e-03	2.33e-03	1.38e-03
τ	1.34e-02	4.37e-05	1.22e-02	4.33e-05	1.08e-02	1.13e-02	9.73e-03	2.94e-05	1.08e-02	2.82e-05
A_s	5.45e-11	4.82e-12	4.94e-11	4.77e-12	4.39e-11	4.58e-11	3.92e-11	2.83e-12	4.32e-11	2.66e-12

Table 5. Same as table 3, except for ΛCDM parameters.

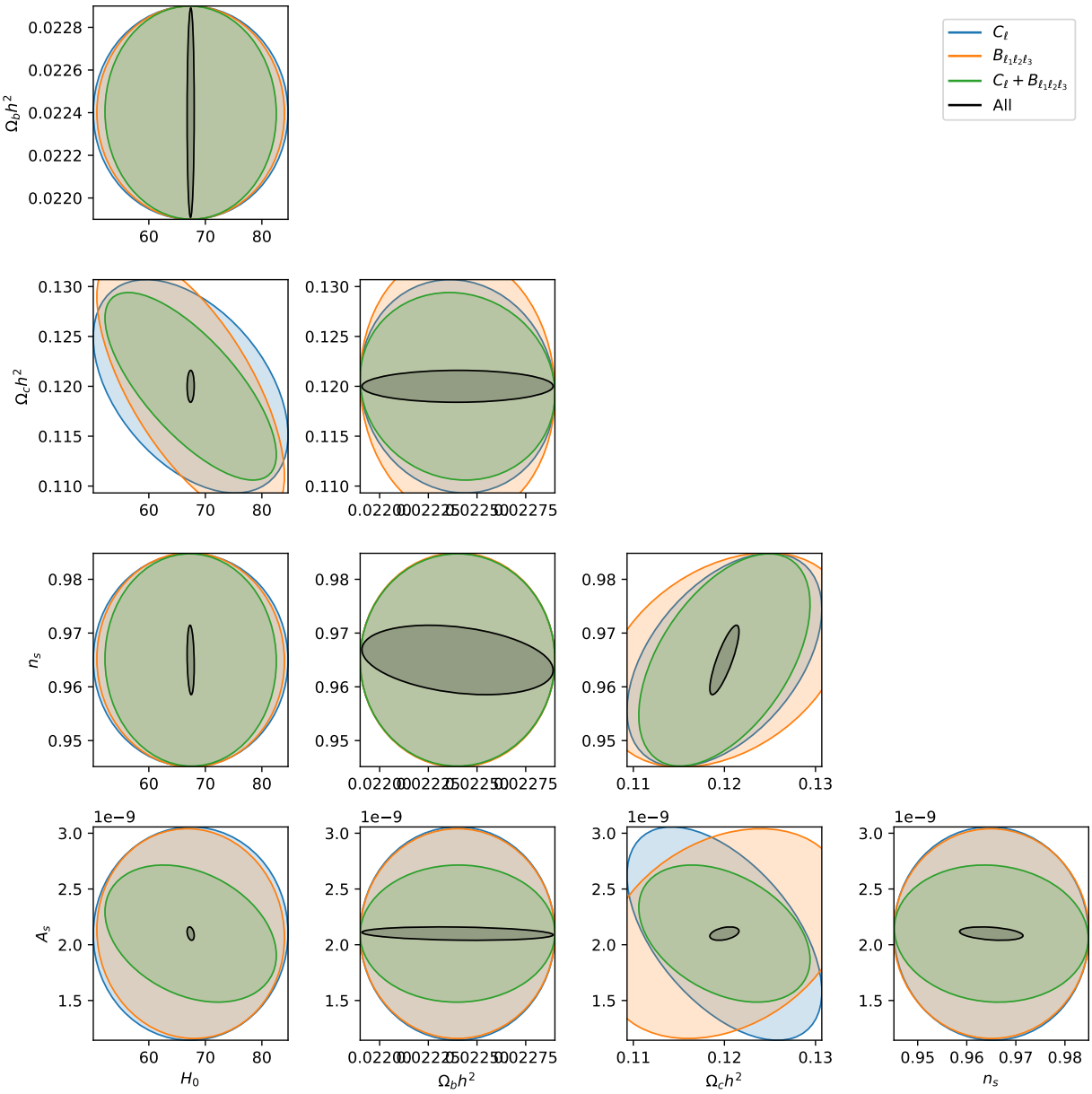

Figure 8. Same as figure 3, except for the standard ΛCDM parameters.

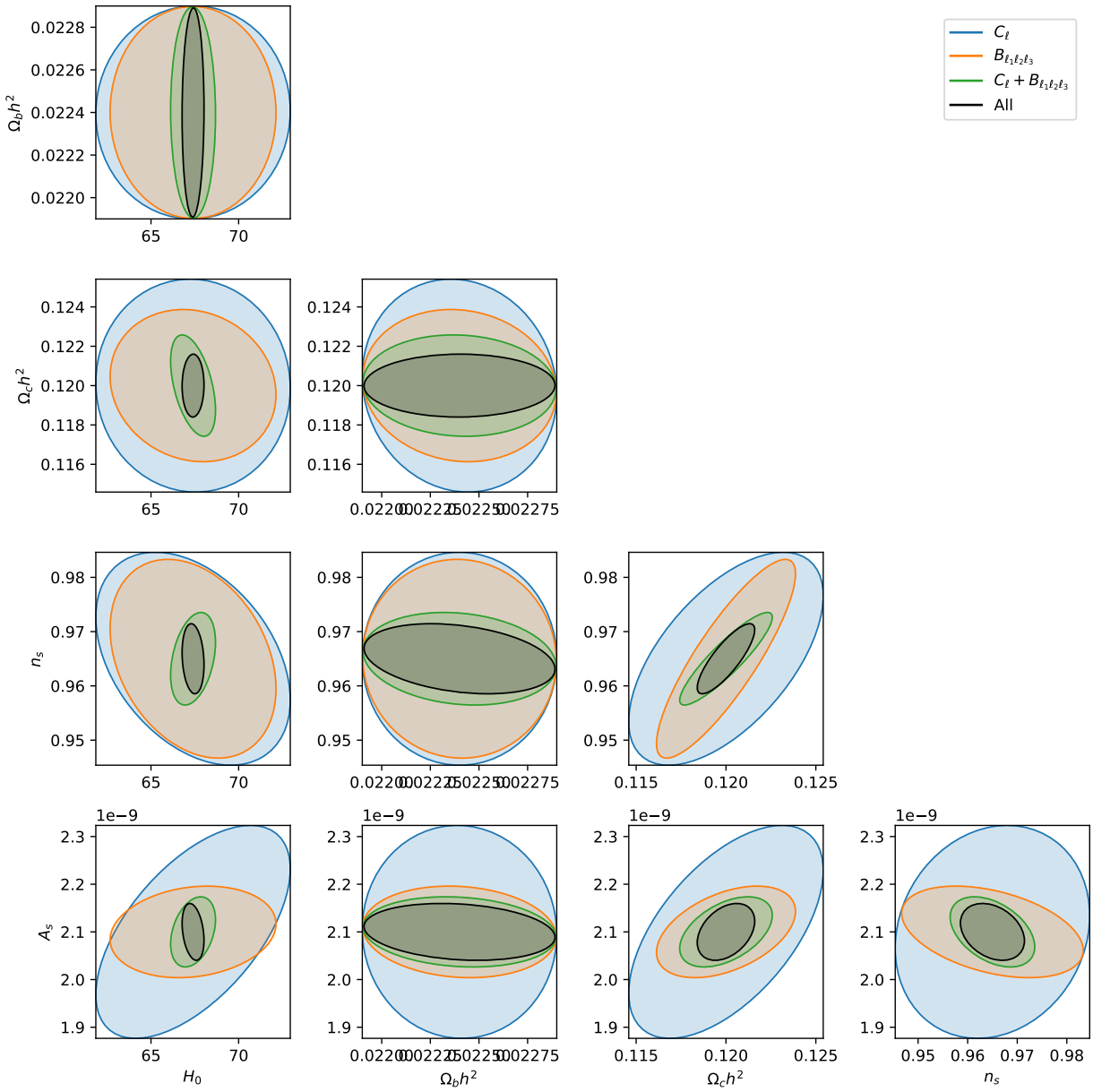

Figure 9. Same as figure 5, except for the standard ΛCDM parameters.